J Neurophysiol 94: 2353–2378, 2005.
First published May 11, 2005; doi:10.1152/jn.00989.2004.

Motor Cortex Neural Correlates of Output Kinematics and Kinetics During Isometric-Force and Arm-Reaching Tasks

Lauren E. Sergio,[1,2] Catherine Hamel-Pâquet,[1] and John F. Kalaska[1]

[1]*Centre de Recherche en Sciences Neurologiques, Département de Physiologie, Université de Montréal, Montreal, Quebec; and*
[2]*Department of Kinesiology and Health Sciences, Bethune College, York University, Toronto, Ontario, Canada*

Submitted 21 September 2004; accepted in final form 8 May 2005

Sergio, Lauren E., Catherine Hamel-Pâquet, and John F. Kalaska. Motor cortex neural correlates of output kinematics and kinetics during isometric-force and arm-reaching tasks. *J Neurophysiol* 94: 2353–2378, 2005. First published May 11, 2005; doi:10.1152/jn.00989.2004. We recorded the activity of 132 proximal-arm-related neurons in caudal primary motor cortex (M1) of two monkeys while they generated either isometric forces against a rigid handle or arm movements with a heavy movable handle, in the same eight directions in a horizontal plane. The isometric forces increased in monotonic fashion in the direction of the force target. The forces exerted against the handle in the movement task were more complex, including an initial accelerating force in the direction of movement followed by a transient decelerating force opposite to the direction of movement as the hand approached the target. EMG activity of proximal-arm muscles reflected the difference in task dynamics, showing directional ramplike activity changes in the isometric task and reciprocally tuned "triphasic" patterns in the movement task. The apparent instantaneous directionality of muscle activity, when expressed in hand-centered spatial coordinates, remained relatively stable during the isometric ramps but often showed a large transient shift during deceleration of the arm movements. Single-neuron and population-level activity in M1 showed similar task-dependent changes in temporal pattern and instantaneous directionality. The momentary dissociation of the directionality of neuronal discharge and movement kinematics during deceleration indicated that the activity of many arm-related M1 neurons is not coupled only to the direction and speed of hand motion. These results also demonstrate that population-level signals reflecting the dynamics of motor tasks and of interactions with objects in the environment are available in caudal M1. This task-dynamics signal could greatly enhance the performance capabilities of neuroprosthetic controllers.

INTRODUCTION

Despite years of study, a broad consensus on the nature of the motor representation expressed by the discharge of primary motor cortex (M1) neurons remains elusive. Correlations have been described between neuronal activity and the static and dynamic forces and torques generated across single joints (Ashe 1997; Cabel et al. 2001; Cheney and Fetz 1980; Evarts 1968, 1969; Humphrey et al. 1970; Thach 1978), or by the whole arm (Ashe 1997; Georgopoulos et al. 1992; Kalaska et al. 1989; Li et al. 2001; Sergio and Kalaska 1997, 2003; Taira et al. 1996), and during precision-pinch tasks (Hepp-Reymond et al. 1999; Maier et al. 1993; Smith et al. 1975). Other studies have reported correlations between neuronal discharge and muscle activity (Bennet and Lemon 1994, 1996; Cheney et al. 1985; Fetz and Cheney 1980; Holdefer and Miller 2002; Lemon and Mantel 1989; Morrow and Miller 2003; Park et al. 2004; Poliakov and Scheiber 1999). These findings suggest that M1 functions at a level near the final motor output to muscles.

In contrast, other studies have described relationships between M1 activity and various kinematic parameters of motor output such as the direction and distance of targets relative to the hand, and the direction, speed, and spatial path of hand displacement (Ashe and Georgopoulos 1994; Caminiti et al. 1990, 1991; Georgopoulos et al. 1982, 1983, 1988; Kalaska et al. 1989; Fu et al. 1993, 1995; Moran and Schwartz 1999a,b; Reina et al. 2001; Schwartz 1992, 1993, 1994; Schwartz and Moran 1999; Schwartz et al. 1988, 2004). These results suggest that M1 functions at a higher level in the putative motor control hierarchy further removed from the motor periphery and generates a descending motor command that defines the spatio-temporal form of the action to perform (its kinematics) rather than how it should be performed (its kinetics).

A related controversy concerns the parameter spaces and coordinate frameworks in which motor output is encoded in M1. This debate focuses on the degree to which activity is related to extrinsic spatial attributes of motor output or to intrinsic limb-, joint-, or muscle-centered parameters (Caminiti et al. 1990, 1991; Kakei et al. 1999, 2001, 2003; Scott and Kalaska 1997; Sergio and Kalaska 1997, 2003) and whether the reference frame is centered on the hand or on other parts of the limb (Cabel et al. 2001; Caminiti et al. 1990, 1991; Moran and Schwartz 1999a,b; Reina et al. 2001; Schwartz 1992, 1993, 1994; Scott and Kalaska 1997; Sergio and Kalaska 1997, 2003). Other findings suggest that the nature and point of origin of the framework may even vary with time during the planning and execution of a motor action (Fu et al. 1993, 1995; Scott and Kalaska 1996, 1997; Sergio and Kalaska 2003; Shen and Alexander 1997a,b; Zhang et al. 1997).

The interpretation of neurophysiological findings is further confounded by the continuing theoretical controversy over the computational architecture of the motor system, in particular whether it uses force control or position control to produce desired motor outputs. Force-control schemes assume that after defining the kinematics of the desired motor output but before emitting any control signals that specify the necessary muscle activity patterns, the motor system generates an intervening representation of the required causal forces or joint-centered torques (Bhushan and Shadmehr 1999; Haruno et al. 2001;

Address for reprint requests and other correspondence: J. F. Kalaska, Centre de Recherche en Sciences Neurologiques, Département de Physiologie, Université de Montréal, C.P. 6128, Succursale Centre-ville, Montréal, Québec, Canada H3C 3J7 (E-mail: kalaskaj@physio.umontreal.ca).

The costs of publication of this article were defrayed in part by the payment of page charges. The article must therefore be hereby marked "*advertisement*" in accordance with 18 U.S.C. Section 1734 solely to indicate this fact.

Hollerbach 1982; Nakano et al. 1999; Schweighofer et al. 1998; Todorov 2000; Uno et al. 1989; Wolpert and Kawato 1998). A force-control architecture requires the motor system to possess implicit or explicit knowledge of the laws of motion and the dynamical properties of the limb and the environment, and to perform a neuronal equivalent of the notorious "inverse-dynamics" transformation in Newtonian mechanics. In contrast, position control schemes (e.g., Bizzi et al. 1984; Feldman 1986; Feldman and Levin 1995; Polit and Bizzi 1979) do not require the supraspinal motor system to generate an explicit representation of task dynamics or descending motor commands that explictly signal output forces or muscle contractile activity patterns. For instance, the "λ" (lambda) model of "equilibrium-point" control (Feldman 1986; Feldman and Levin 1995; Feldman et al. 1990; Gribble and Ostry 1999, 2000; Ostry and Feldman 2003) achieves the inverse transformation between desired kinematics and causal muscle activity indirectly by descending control of spinal motoneuron recruitment thresholds, to drive the arm to a new posture at which internal and external viscoelastic forces are at equilibrium.

Beyond their theoretical significance, these issues have taken on added practical importance because of rapid advances in neuroprosthetic technologies that use the recorded activity of M1 neurons to control robotic devices (Carmena et al. 2003; Serruya et al. 2002; Taylor et al. 2002). These controllers typically use decoding algorithms that extract signals about desired kinematics (e.g., position, direction, velocity) (Paninski et al. 2004a,b), and do not cope readily with abrupt changes in the dynamics of motor tasks (Carmena et al. 2003). The performance of neuroprosthetic controllers could be improved by a deeper understanding of the motor representation in M1.

The present study examines the degree to which M1 activity reflects the kinematics or kinetics of whole-arm motor tasks. Monkeys alternately performed either a whole-arm isometric force task or a reaching task to displace a cursor between targets on a monitor screen. The cursor motions reflected the direction of motor outputs measured at the hand and imposed the identical global behavioral constraint on performance in both tasks. However, the output parameter used to control cursor motion differed between tasks. In the isometric task, the monkeys used their arm to generate force ramps at the hand in eight directions in a horizontal plane, and the cursor provided feedback of hand-centered forces. The direction and time course of the behavioral constraint (cursor motion) and of the causal forces at the hand were co-linear and isomorphic at all times. In the movement task, the monkeys made ramp displacements of the hand in the same eight horizontal directions to move a weighted pendular handle, and the cursor provided hand position feedback. The monkeys had to generate complex patterns of horizontal output forces at the hand to compensate for the inertial load imposed by the pendulum. Unlike the isometric task, however, the causal horizontal forces were not the output variable controlled by the task, they were not displayed on the monitor, and their directionality was transiently dissociated from hand displacement and cursor motion as the hand approached the targets.

The activity of many single neurons and the net population signal in the caudal part of M1 reflected the large differences in the time course and directionality of output dynamics between the two tasks to a much greater extent than they did the large differences in the output kinematics or the similarity in the global behavioral constraints of the two tasks. Preliminary results have been reported previously (Sergio and Kalaska 1998).

Note that terms borrowed here from mechanics (e.g., kinematics, kinetics, dynamics) have specific and at times variable meanings in that field. They are used here only as convenient descriptors to express the degree to which neuronal activity covaries with the externally observable spatiotemporal form of motor outputs (task "kinematics"), or to their underlying causal forces, torques, and muscle activity (task "kinetics"), while the system is in equilibrium (task "statics") and especially while in transition between static states (task "dynamics"). These terms clearly have implications for the nature of the motor representation in M1, but their use here should not be interpreted as support for the explicit coding of any particular Newtonian mechanical parameter by the activity of M1 neurons.

METHODS

Task apparatus

Two juvenile male rhesus monkeys (*Macaca mulatta*; 3.4–7.0 kg, 3.4–6.1 kg) were trained to perform isometric-force and arm-movement tasks. In the isometric task, the monkeys grasped a 20-mm-diameter ball on the end of a 65-mm vertical rod that was attached to a 6df (degree-of-freedom) force/torque transducer (Gamma F3/T10; Assurance Technologies) placed in a fixed position in front of them (Sergio and Kalaska 1997, 2003). They used their whole arm to exert forces against the rigid rod. The rod passed freely through a small hole in a thin metal plate that was attached by hinges to the top edge, furthest away from the monkey, of a box that housed the transducer. The free end of the plate sat on a microswitch. If the monkey rested its hand on the plate or applied forces to it, the switch would close and halt the task. This ensured that all force outputs at the hand were applied only to the rod and were sensed by the transducer.

In the movement task, an identical rod/transducer/housing assembly was attached to the end of a 1.6-m-long pendulum. The complete assembly weighed 1.3 kg (see *Behavioral tasks* below), and the pendulum plus transducer was 2.6 kg. This imposed a large inertial load during movement, unlike other studies in our lab (Cisek et al. 2003; Crammond and Kalaska 1996, 2000; Kalaska et al. 1989; Scott and Kalaska 1997). A sonic digitizer (GP-9; Science Accessories) measured the X–Y position of the pendulum base at 55 Hz with a resolution of 0.1 mm.

A computer monitor was positioned at eye level 60 cm in front of the monkeys. In the isometric task, a cursor on the monitor gave continuous feedback of the current force level applied to the force transducer in the X–Y (horizontal) plane, sampled at 200 Hz. The X-axis was aligned to the 0–180° (*right–left*) direction in front of the monkeys, and the Y-axis to the 90–270° direction (Fig. 1). In the movement task, the cursor gave position feedback about the current spatial location of the pendulum. The X–Y forces applied to the handle were also sampled at 200 Hz but were not displayed. In both tasks, the monkeys' starting hand location was at the midline, 20 cm in front of the sternum, approximately level to the zyphoid process.

Behavioral tasks

At the start of each trial of the isometric task, a circle appeared at the center of the monitor (Fig. 1). The monkeys had to generate a small static bias force (0.3 N) away from the body to position the cursor within the central force target for a variable (1–3 s) hold period. The central target then disappeared and a peripheral force target (diameter: 0.28 N) appeared at one of eight locations arrayed in a circle around the central target. The separation of the centers of the central and peripheral targets corresponded to a 1.5 N change of force.

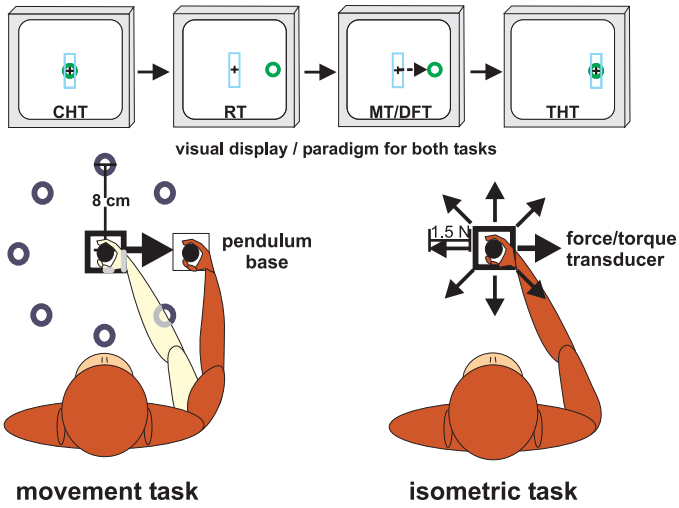

FIG. 1. Experimental setup and task apparatus used in the study. *Top row*: time sequence of stimulus events viewed by the monkey on a monitor screen during a single trial of the 2 tasks. Monkey initiated a trial by positioning a cursor ("+") in a central green target circle while maintaining vertical forces within acceptable limits (blue box, see text). "GO" signal was the simultaneous presentation of a peripheral target circle and disappearance of the central circle. Monkey generated an isometric force ramp or arm movement to displace the cursor into the target and held it there for 2 s. *Bottom row*: *top view* of the monkey performing the movement (*left*) and isometric (*right*) tasks. Open circles on *left* illustrate the spatial locations of the peripheral targets in the horizontal plane the movement task. Note that no targets were physically present in the horizontal workspace of the movement task, and performance was guided entirely by cursor motions on the monitor in both tasks. Squares represent the housing of the force–torque transducer of the instrumented manipulanda in each task. Monkeys grasped a knob (solid circle) at the end of a rod on the manipulanda to displace the task handle (*left*) or generate isometric forces (*right*) to displace the cursor on the monitor.

The monkeys generated a force ramp in the indicated direction in the horizontal plane to move the cursor into the peripheral target, and held it there for 2 s to receive a liquid reward (Fig. 2*A*). The animals generated force ramps aimed at each target from their onset, and did not initially relax the bias force. Targets were spaced at 45° intervals, starting from 0° (to the *right*) and progressing counterclockwise. The eight targets were repeated five times in a randomized-block design. The same event sequence was followed in movement-task trials, but the cursor provided pendulum position feedback. The monkeys had to generate a bias force to push the pendulum from its suspended rest position away from the body by 2 cm to place the cursor in the central target. Movements of 8 cm were required to displace the cursor from the central to the peripheral targets. Extra weights were added empirically to the transducer assembly to ensure similar ranges of static and dynamic forces in the two tasks (Fig. 2). The mean change in static force relative to the central target exerted by the monkeys to hold the pendulum at the peripheral targets (about 1.0 N) was less than the static forces in the isometric task. However, increasing the pendulum's mass to require final static forces of 1.5 N increased the inertial load to such a degree that the dynamic accelerative and braking forces became far larger than any forces in the isometric task. It also made it very difficult for the monkeys to respect the behavioral constraints of movement timing, endpoint accuracy, and vertical forces (see following text) to ensure reliable and willing performance of the movement task. However, exact duplication of the range of dynamic and static forces in the two tasks was not essential in this study because its objective was not to make a quantitative comparison of the parametric coding of specific output force levels in the two tasks.

The monkeys also received continual feedback about the forces generated at the hand in the vertical (Z) axis in both tasks. A rectangular box was drawn about the cursor (Fig. 1) and moved with it on the monitor as the monkeys generated horizontal forces or movements. The vertical position of the box relative to the cursor signaled the measured vertical forces. A small constant vertical offset in the display of the box required a 0.3-N downward force to center the cursor in the box. This allowed the monkeys to rest their hand gently on the handle while performing the tasks. The vertical length of the box indicated the acceptable range of vertical forces (0.26 N for monkey A; 0.5 N for monkey B) about the constant vertical offset. If the Z-axis forces exceeded that range, the box shifted to a point where the cursor was no longer inside it, and the trial stopped. This extra behavioral control ensured that the output forces generated by the monkeys at the hand were confined to a narrow vertical range about the horizontal plane and prevented them from systematically varying the vertical component of the output forces as a function of direction or task, which would confound the interpretation of cell activity.

Data collection

The animals were trained to >80% success rates in both tasks. They were then prepared for neuronal recordings in M1 using standard aseptic surgical techniques (Kalaska et al. 1989).

Conventional techniques were used to record the activity of single M1 neurons (Kalaska et al. 1989). During each recording session, a microelectrode was advanced through the cortex while the animal performed the tasks. When a neuron was isolated, its task-related responses were tested initially by performing a few trials in several directions. Its passive responses were tested by manipulating the arm joints, brushing the skin, and palpating muscles. The arm was also observed for signs of movements or muscle contractions during low-threshold intracortical microstimulation (ICMS) of the cortex. A neuron was selected for further study if this evidence indicated that it was related to movements of the contralateral shoulder and/or elbow but not to more distal joints, and it displayed directional tuning in at least one of the tasks. Attempts were made to record neurons from all cortical layers but the need for stable isolation over long periods of time (Sergio and Kalaska 1997, 1998, 2003) led to a bias toward neurons with large-amplitude extracellular spike waveforms recorded in intermediate cortical layers.

The monkeys performed data files of 40 trials first in one task and then the other. The order in which the tasks were performed varied from neuron to neuron, and duplicate sets of data files were sometimes collected from the same neuron to ensure repeatability of results.

In both monkeys, activity was recorded from 16 proximal-arm muscles in separate recording sessions. Muscles were implanted percutaneously with pairs of Teflon-insulated 50-μm single-stranded stainless steel wire electrodes. Implantations were verified by stimulation through the wires to evoke muscle contractions (<1.0 mA, 30 Hz, 300-ms train). Multiunit EMG activity was amplified, band-pass filtered (100–3,000 Hz), half-wave rectified, integrated (5-ms bins), and digitized at 200 Hz. The muscles studied were the biceps brachii, brachialis, anterior deltoid, middle deltoid, posterior deltoid, dorsoepitrochlearis, infraspinatus, latissimus dorsi, pectoralis, subscapularis, supraspinatus, teres major, rostral trapezius, caudal trapezius, triceps longus, and triceps medialis. These recordings were done only to assess the behavior of the muscles in the two tasks, to provide a benchmark against which to compare cell activity. They were not intended as a definitive quantitative study of the response properties of each muscle.

Near the end of recordings in each cylinder, small electrolytic lesions were made (5–10 μA, 5 s) in selected penetrations. At the conclusion of the experiment, the monkeys were deeply anesthetized with barbiturates and perfused with buffered saline and formalin (monkey A) or saline and 4% paraformaldehyde (monkey B). Pins were inserted into the cortex at known grid coordinates to delimit the area from which cell recordings were made and the cortex was sectioned to permit localization of the marked penetrations.

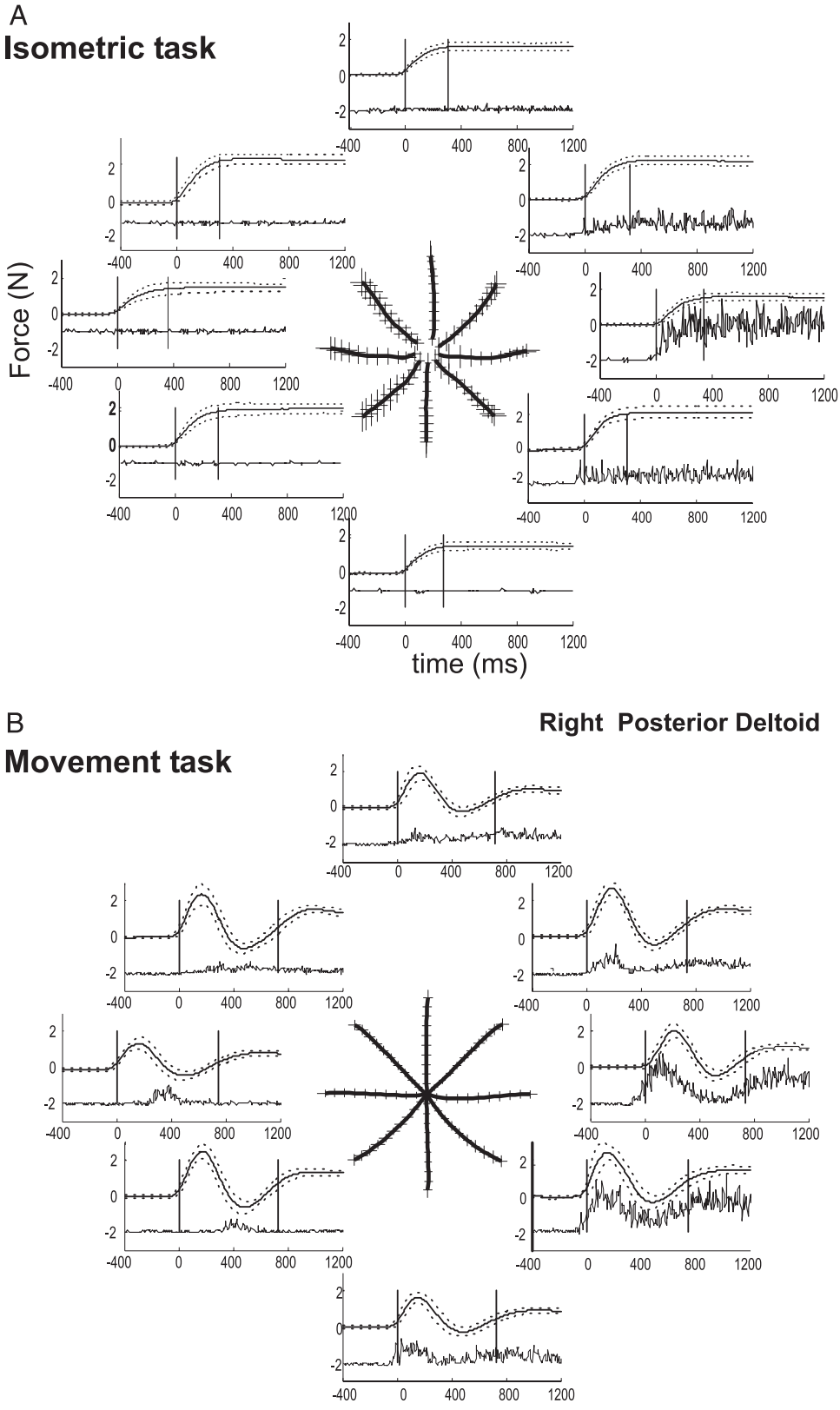

FIG. 2. *A*: histograms show the averaged electromyographic activity (EMG) of the right posterior deltoid muscle recorded during 5 trials of isometric force production in each of 8 directions. The average temporal force profile at the hand in each force direction, above each EMG histogram, shows the change in the average length of the component of the force output vector aligned along the direction of the target force at each moment in time, relative to the mean bias–force vector during center hold time (CHT). Data are oriented to the onset of dynamic force time (DFT) (*time 0*, *left solid vertical line*). *Right vertical line* denotes the average end of DFT and beginning of target hold time (THT) across trials at each force direction. Mean X–Y force paths are shown at the *middle* (crosses denote SDs at 20 equidistant points along the paths). *B*: EMG activity from the same muscle during the movement task. Average temporal force profile for each movement direction is shown above the muscle activity. *Middle*: displays the average X–Y movement hand path in the horizontal plane (with SDs shown at 20 equidistant points).

Data analysis

Four behavioral epochs were defined in both tasks. Center hold time (CHT) ended when the peripheral target appeared. Reaction time (RT) was the interval between the appearance of the peripheral target and the first detectable change in force measured by the transducer in both tasks. Movement time (MT, movement task) or the equivalent dynamic force time (DFT, isometric task) ended when the controlled motor output stabilized at either a constant spatial position (movement task) or static force level (isometric task) within the peripheral target.

Target hold time (THT) was the remaining period of static hold in the target. Single-trial spike rates were calculated for each epoch using the whole and partial spike intervals that fell within the epoch, rather than simple spike counts (Georgopoulos et al. 1982, 1988; Sergio and Kalaska 2003; Taira et al. 1996). A leading partial spike interval is defined as the fraction of the whole spike interval between the first spike in the epoch and the last spike that occurred before the epoch started that falls within the epoch. A trailing partial spike interval is the fraction of the whole spike interval between the last spike in the epoch and the first spike occurring after the epoch that is contained within the epoch. If no spikes occur in an epoch, the partial spike interval is the duration of the epoch divided by the interval between the last spike before and the first spike after the epoch. The epoch spike rate (s/s) is the sum of the leading and trailing partial spike intervals and the whole intervals between consecutive spikes within the epoch itself, normalized for the epoch duration. This approach yields a more continuous distribution of spike rates than spike counts and provides a more accurate measure of activity by accounting for the entire time period of interest in the spike train within which it is embedded (Taira et al. 1996).

An unbalanced repeated-measures ANOVA was used to test for a significant main effect of direction and task, and for direction-task interactions ($P < 0.01$, 5V program, BMDP Statistical Software, University of California, Los Angeles, CA) in all epochs.

The electromyographic (EMG) activity recorded from proximal-arm muscles was subjected to the same analyses as the cells. Whenever analyses required the pooling of results from different cells or muscles, all data collected while the monkeys performed the task with the left arm were subjected to a mirror-image transformation about the 90–270° (Y) axis.

TIME COURSE OF CHANGES IN DIRECTIONAL TUNING. A temporal analysis was made of the evolution of each neuron's directional tuning during the trials. Spike data were aligned to the moment of force onset in each trial in both tasks. A 50-ms sliding window was advanced in 10-ms steps, from 400 ms before force onset to 1,200 ms after force onset, and tests were performed on the directional tuning of the windowed activity at each step, as follows.

The discharge rate was calculated within the 50-ms window at a given time step t in each trial, using whole and partial spike intervals. Discharge rates were not transformed further. The 40 samples of windowed activity in each task were tested for a significant relation to direction (ANOVA, $P < 0.01$), and the preferred direction (PD) of the windowed activity at time t was calculated for the movement (PD_{mt}) and isometric (PD_{it}) tasks. The data were also tested using a bootstrap method with random shuffling of data across directions to assess whether the directional tuning could have occurred by chance (Georgopoulos et al. 1988; Sergio and Kalaska 1998, 2003).

Next, the angular difference (ΔPD_t) between PD_{mt} and PD_{it} was calculated for all cases of significant directional tuning in a given time window for both tasks. A second bootstrap procedure was used to assess whether the observed ΔPD_t was significant or could have occurred by chance. This test assumed that if the tuning function of a neuron is the same in the two tasks, then the distribution of ΔPD_t calculated from multiple samples of neuronal activity in the two tasks will be centered on 0° angular difference. To implement this test, we generated an estimate of the directional tuning curve of the cell in the movement task by random selection, with replacement, of five values of the discharge rate of the cell from the sample of five single trials at each of the eight directions. Data were not shuffled across directions for this test. The PD of this bootstrapped sample of data (PD_{mtb}) was calculated by standard methods. This was repeated for the data in the isometric task to calculate a PD_{itb}. The signed difference ΔPD_{tb} between PD_{mtb} and PD_{itb} was calculated. This was repeated 1,000 times to generate a distribution of ΔPD_{tb} values, which were rank ordered. The limits of the 95% confidence interval (CI) were defined as the 25th and 975th largest ΔPD_{tb} values (two-tailed test). A neuron was considered to have a significant difference in PD between the two tasks in a given time window if it was: *1*) significantly directionally tuned in both tasks and *2*) the value of 0° fell outside of the 95% CI of the distribution of bootstrapped ΔPD_t (i.e., the null hypothesis that the observed value for ΔPD_t was not significantly different from 0° can be rejected at $P < 0.05$, two-tailed test). This test was also used to compare the directional tuning of each neuron at different times in the same task.

POPULATION-VECTOR ANALYSIS. To examine the directional correspondence between overall M1 activity and the motor output as a function of time, a population-vector analysis was performed on neuronal activity in nonoverlapping 20-ms bins, aligned to force onset in each trial, from 400 ms before force onset to 1,200 ms after force onset. The population vector **P** for a given direction of motor output **d** at a given moment in time **t**, was calculated in standard fashion as

$$\mathbf{P_{dt}} = \Sigma W_{dti} \cdot PD_i, \quad \text{with} \quad W_{dti} = f_{dti} - cht_i \qquad (1)$$

where PD_i is the preferred direction of the ith cell in the sample and W_{dti} is its weighted discharge rate, calculated as the difference between its binned discharge rate f_{dti} for direction d at time t, and its mean center-hold tonic discharge rate cht_i while generating the static offset bias forces in both tasks before the appearance of a peripheral target. Spike rates were calculated using whole and partial intervals. Hand-centered forces and kinematics were also analyzed every 20 ms.

Each population vector is the sum of the vectorial contribution of all neurons along their own PD. However, the calculated PD of a neuron can change between windows, in part because the stochastic nature of its activity is accentuated when examined in short time windows from small data samples (40 trials). Furthermore, the windowed activity of muscles and neurons often showed large changes in apparent PD during the MT epoch of the movement task (Sergio and Kalaska 1998; see RESULTS). This raises the question of how to define the directional influence of a given neuron at a given moment in time, and thus its contribution to the population signal.

To address this question, we assumed that the directional influence exerted by each neuron on motor output remains stationary, at least over the time frame of single trials and single data files. The directional tuning of single muscles and M1 neurons was generally similar in the two tasks for the mean activity during the RT and especially the THT epochs. Therefore we calculated the PD of the M1 neurons using their mean activity during the THT epoch in each task, and used it as the canonical PD of the neuron for each 20-ms window of that task. Using the PD during the RT epoch did not fundamentally alter the basic findings of this analysis.

RESULTS

Database

Task-related activity was recorded from 132 cells in both tasks during 134 penetrations in the primary motor cortex (M1) of three hemispheres from two monkeys (71 and 17 cells from the left and right hemispheres of monkey A, 44 cells from the right hemisphere of monkey B). These monkeys were also used to study the effects of changes in arm posture on isometric force–related M1 activity (Sergio and Kalaska 1997, 2003), and most of the neurons in that study form part of the present data set. Almost all neurons were recorded from the most caudal part of M1 in the anterior bank of the central sulcus. To be included in the data sample, a neuron had to be related to movements of the proximal arm and directionally tuned during at least one trial epoch in one of the tasks. As in previous studies (Crammond and Kalaska 1996; Kalaska et al. 1989; Scott and Kalaska 1997; Sergio and Kalaska 2003), the sample

was biased toward neurons related to movements of the shoulder and shoulder girdle. Some neurons were related primarily to the elbow. Any neurons related to wrist or hand movements were not retained. All sampled neurons were active in both tasks. This was also true for the many neurons that met the inclusion criteria for the study but were lost before data collection was completed. There was no evidence of significant populations of neurons that were selectively activated in only one of the two tasks.

Task performance

The monkeys produced similar smooth ramplike X–Y trajectories of the experimentally controlled variable in each task, hand-centered forces in the isometric task, and hand positions in the movement task, to displace the cursor from the central to the peripheral targets (Fig. 2).

In contrast, the temporal profile of the forces measured at the hand differed between tasks. A temporal force profile was calculated as the moment-to-moment change in length of the vector component of the measured force output vector that was aligned along the axis of target direction, averaged across all trials in that direction, relative to the mean bias–force vector during CHT in both tasks. In the isometric task, the force profile was a monotonic ramp increase in the direction of the target (Fig. 2*A*). The force profile in the movement task was more complex, including an initial accelerating pulse in the desired direction of motion, a smaller decelerating force in the opposite direction, and a final static force to hold the pendulum over the peripheral target (Fig. 2*B*). The measured deceleration force was smaller than the acceleration force, attributed in part to the decelerating effect of gravity on pendulum motion. The MT epoch of the movement task was typically about twice as long as the corresponding DFT of the isometric task. This compromise was necessary to ensure comparable ranges of measured dynamic output forces in the two tasks and reliable performance of the movement task.

Muscle activity: general description

The differences in force profile were paralleled by task-related changes in muscle activity. In the isometric task, muscles showed a ramp increase in activity, beginning about 50 ms before force onset, across a range of force directions centered on its preferred direction and a decrease or complete suppression of activity in the opposite directions (Figs. 2*A* and 4*A*).

The EMG pattern was strikingly different in the movement task. Muscles often exhibited the classic "triphasic" burst pattern. This involved an initial burst of activity before movement onset in the muscle's preferred direction, then a decrease or complete pause in activity, followed by a sustained increase in activity after the hand stopped at the peripheral target (Figs. 2*B* and 4*B*). In the opposite direction, a delayed "antagonist" burst would often be generated around the time of peak movement velocity and the reversal of output forces exerted on the pendulum (Figs. 2*B* and 4*B*). The delayed burst was usually preceded by a transient decrease in muscle activity and followed by a sustained decrease during the target-hold epoch. The delayed "antagonist" burst was typically much smaller in amplitude than the initial "agonist" burst of the muscle in its preferred direction (Figs. 2*B* and 4*B*; Sergio and Kalaska 1998), consistent with the smaller measured decelerating forces. The antagonist burst was more prominent for muscles whose preferred direction was along the lateral (0–180°) axis, such as the deltoids and pectoralis, and less prominent for muscles oriented along the 90–270° axis, such as elbow flexors and extensors.

In both tasks, performance was characterized by reciprocal activation of muscles whose preferred directions were oppositely oriented. There was little evidence of extensive cocontraction of antagonist muscles in these highly practiced monkeys.

Neuronal activity: general description

Neurons showed a broad continuum of responses at their preferred direction in the isometric task, which could be subjectively divided into two patterns. Most (91/132; 69%) showed a large increase in tonic discharge (Fig. 3, *A* and *C*), often with a strong phasic burst of activity at the leading edge of the tonic increase before force onset (Fig. 4*C*). Other neurons emitted mainly a phasic burst, with little or no change in tonic activity after completion of the force ramp (30/132, 23%). Eleven neurons were unclassifiable. Typically, neurons showed a reciprocal suppression of activity during isometric force production in the opposite direction (Figs. 3*C* and 4*C*).

The response pattern of neurons usually changed in the movement task (Figs. 3, *B* and *C* and 4*D*). Most neurons (80/132, 61%), of any response pattern in the isometric task, displayed a "triphasic" response profile in the movement task, with an initial phasic burst in their preferred direction, followed by a brief pause and then a sustained tonic activity increase that often began with a second, postpause burst of activity. The neurons often displayed a reciprocal pattern in the opposite direction, including a delayed phasic burst during the movement and a decrease in tonic activity during the target-hold epoch (Figs. 3, *B* and *C* and 4*D*). The next largest group (26/132, 20%) showed primarily a phasic response at their PD, whereas 17 other neurons (13%) were tonic, five (4%) were tonic with an initial phasic overshoot but without a transient pause, and three neurons were unclassifiable.

Although the details and timing of the responses varied between neurons, the task-related changes in activity typically paralleled and led in time the differences in force profiles between tasks (Figs. 3 and 6; see later sections).

Although both muscles and neurons showed response components that paralleled the patterns of output forces in both tasks, there were also significant differences between muscle and neuronal activity. The first was the initial phasic burst at the onset of the response of many neurons near their PD in the isometric task (Fig. 4*C*). A corresponding overshoot was never seen in the force outputs (Fig. 2*A*) or in muscles, which showed only gradual increases in contractile activity whose time course paralleled and led the ramp increase in forces (Figs. 2*A* and 4*A*). Second, the delayed "antagonist" bursts of neuronal activity were often almost as strong as, or even stronger than, the initial "agonist" burst in the preferred direction (Figs. 3, *B* and *C* and 4*D*; Sergio and Kalaska 1998). Such strong antagonist bursts were never observed in the muscle activity, which were always much weaker than the muscle's agonist burst in its preferred movement direction (Figs. 2*B* and 4*B*).

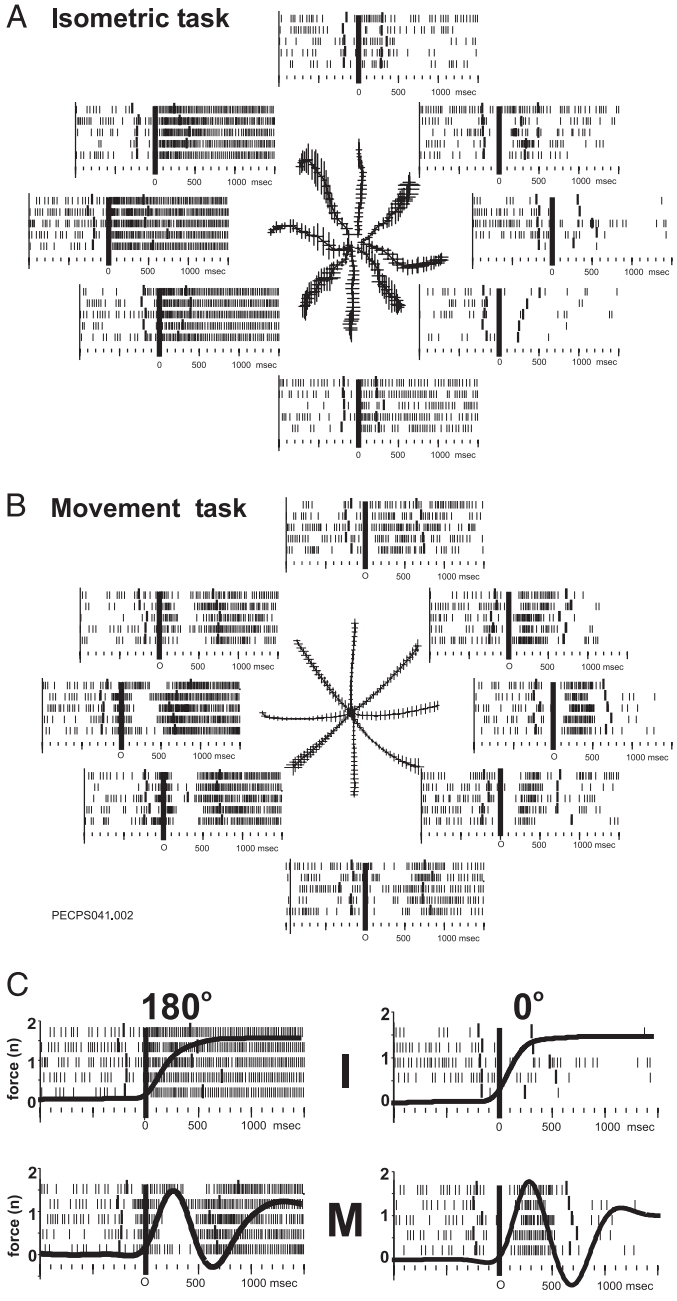

FIG. 3. *A* and *B*: discharge pattern of an M1 neuron during isometric force production (*A*) and arm movement (*B*). Eight rasters in *A* and *B* show activity during 5 trials for one force or movement direction, and each raster location corresponds to the direction of force or movement production away from the starting central target. Data are oriented to the time of force onset at the beginning of the DFT or movement time (MT) epoch, denoted by a solid vertical line at *time 0*. For each trial raster, the taller tick mark to the *left* of force onset shows the time of target onset, whereas the taller tick mark to the *right* shows the time at which motor output stabilized within the peripheral force or movement target (start of THT). Rasters surround the mean force or movement path for the 5 trials in each spatial direction for that data file. *C*: raster displays of the same neuron's activity at its preferred output direction (180°) and the opposite direction (0°) in the isometric ("I") and movement ("M") task, redrawn with the mean temporal force profile for those 5 trials superimposed. Neuron became directionally tuned 50 ms before force onset in the isometric task (obscured by the vertical line) and 120 ms before force onset in the movement task.

ANOVA of activity in different trial epochs

A repeated-measures ANOVA was performed on mean discharge rates during different trial epochs to assess the overall effect of task and direction on neuron and muscle activity (Table 1). Significant main effects of task and direction were prominent in all post-GO trial epochs, but were less common in RT than in later epochs. Most notably, however, the number of neurons that showed a significant task-direction interaction increased sharply from 23% in RT to 88% in MT/DFT and 79% during THT. Muscle activity showed similar trends (Table 1).

A significant interaction implies a difference in directional tuning as a function of task, which can confound the interpretation of significant main effects in the ANOVA. It can express itself in two different but nonexclusive ways (Scott and Kalaska 1997). The depth of a neuron's directional tuning curve could change between tasks. Alternatively, the preferred direction could change between tasks. The following analyses evaluated both possible interaction effects.

The effect of task on dynamic range of activity in different behavioral epochs

To test for task-dependent changes in the depth of a neuron's directional tuning curve independent of any directional shift, we calculated the neuron's dynamic range (DR) of activity in both tasks. The DR was defined as the difference in activity between the two directions of motor output that evoked the maximum and minimum mean discharge rates in a given task.

Figure 5, *A–C* shows scatter plots of single-neuron DRs between tasks for each trial epoch. The DR distribution was shifted toward significantly smaller values during the MT epoch of the movement task than during the DFT period of the isometric task (mean DR: 24.4 vs. 31.7 imp/s, respectively; paired *t*-test, $P < 0.01$). In contrast, there were no significant differences in DR distributions between the movement and isometric tasks during the RT (18.4 vs. 18.4 imp/s) and THT (20.8 vs. 19.5 imp/s) epochs. Furthermore, the correlation between the DR of neurons in the two tasks was much weaker during the MT/DFT epoch ($R^2 = 0.11$) than during the RT ($R^2 = 0.46$) and THT ($R^2 = 0.41$) epochs, respectively. Both of these effects on DR during the MT/DFT epoch were likely a result, in part, of averaging the complex changes of neuronal activity across the duration of the MT epoch in each direction of the movement task. This could account for part of the increase in incidence of significant interaction effects between the RT and MT/DFT epochs but not for the continued high incidence in the THT epoch.

Effect of task on directional tuning of activity in different behavioral epochs

Neurons were broadly tuned for the direction of motor output in both tasks (Figs. 3 and 4). The distributions of PDs were statistically uniform in all three trial epochs of both tasks (Rayleigh test, Rao's spacing test, $P > 0.05$; data not shown; Batschelet 1981).

A significant interaction effect could result from a shift in directional tuning between tasks independent of changes in DR. Figure 5, *D–F* shows the distribution of PD differences (ΔPD) for those neurons that were significantly tuned in the

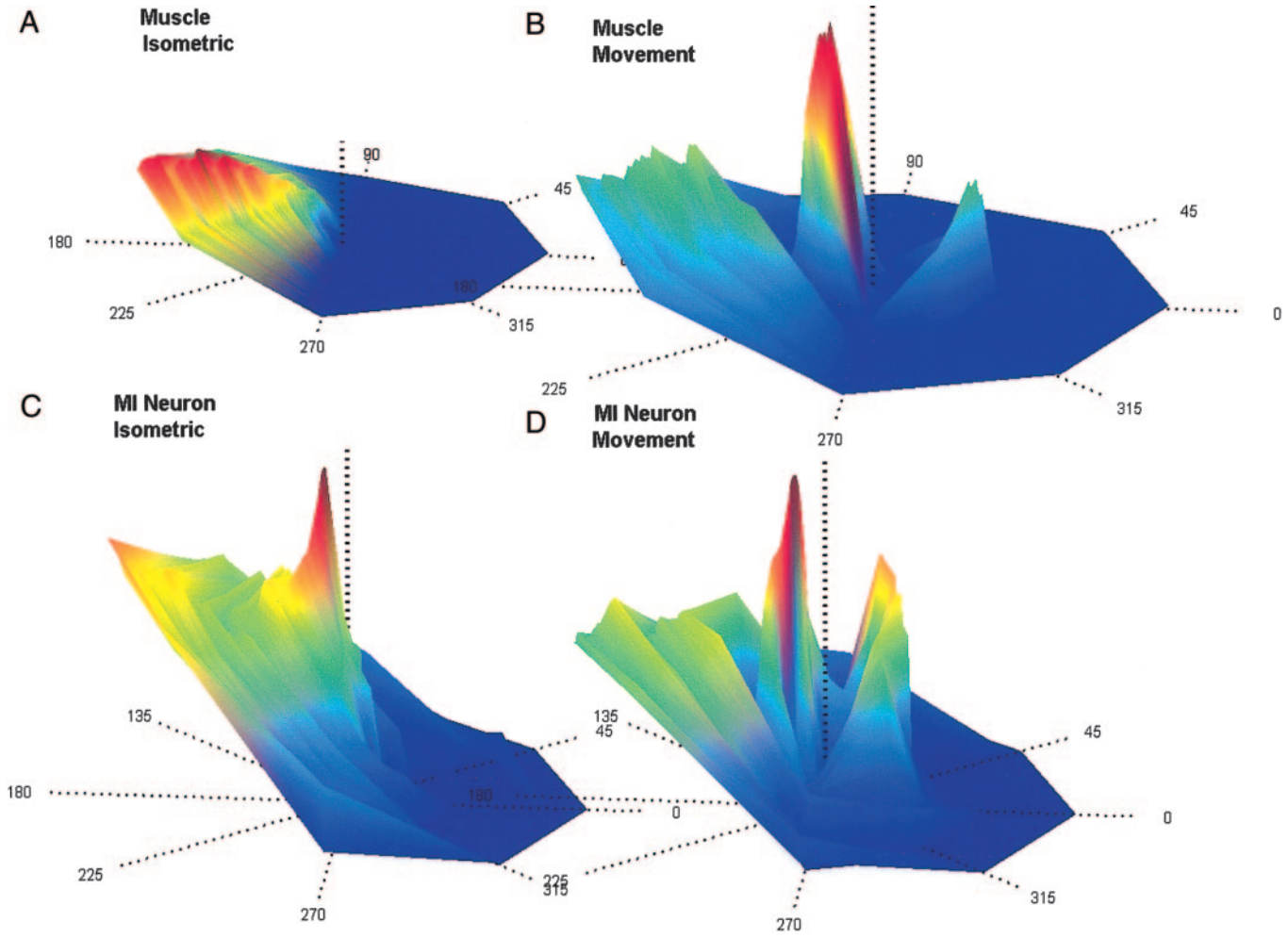

FIG. 4. Three-dimensional (3D) representation of the EMG activity of the right pectoralis muscle as a function of output direction and time from one monkey in the isometric (*A*) and movement (*B*) tasks, and of a different neuron from that shown in Fig. 3 in the isometric (*C*) and movement (*D*) tasks. Data are shown from −200 to +1,400 ms relative to force onset, beginning at the center of the plot. Distance from the center represents time, whereas the height represents cell or muscle activity magnitude. 3D surfaces were generated by interpolation across direction of the neuronal and EMG response histograms for the 8 motor output directions in each task.

two tasks in a given trial epoch. During RT and THT, PDs were similar between the two tasks, as indicated by the strong clustering of data near zero degrees difference (Fig. 5, *D* and *F*). During MT/DFT, in contrast (Fig. 5*E*), there was greater scatter in the distribution of ΔPD. This was once again attributed in part to averaging the complex temporal profile of activity in the movement task across the entire MT epoch. For instance, if a neuron showed a strong delayed antagonist burst in directions of the movement task that were opposite to their PD in the isometric task, this would bias the calculated PD toward that direction and cause a large apparent ΔPD between the two tasks. A bootstrap test was used to assess whether the observed ΔPD between tasks was statistically significant (see METHODS). The incidence of significant ΔPD increased sharply from RT (12/79; 15%) to MT/DFT (68/103; 66%) and then decreased in THT (60/117; 51%) (Fig. 5, *D–F*). This increase in ΔPD also likely accounted for much of the change in incidence of significant ANOVA interaction effects across epochs.

TABLE 1. *Incidence (and %) of significant effects on activity (unbalanced repeated-measures ANOVA, Wald test, $\Delta < 0.01$)*

	Task	Direction	Interaction
Cells (n = 132)			
RT	66 (50)	99 (75)	30 (23)
MT/DFT	96 (73)	129 (98)	116 (88)
THT	83 (63)	126 (95)	104 (79)
Muscles (n = 32)			
RT	16 (50)	24 (75)	14 (44)
MT/DFT	27 (84)	31 (97)	30 (94)
THT	26 (81)	31 (97)	29 (91)

Changes in directional tuning over time within and between tasks

The preceding epoch-based analyses treated neuronal responses as quasi-tonic signals, by averaging the activity of each neuron over several hundred milliseconds in each trial epoch. This masked any finer detail in the temporal pattern of activity.

To study the evolution of directional tuning in greater temporal resolution, we performed directional tests on a sliding 50-ms window of activity, incremented in 10-ms steps, aligned to force onset in each trial (see METHODS). The instantaneous

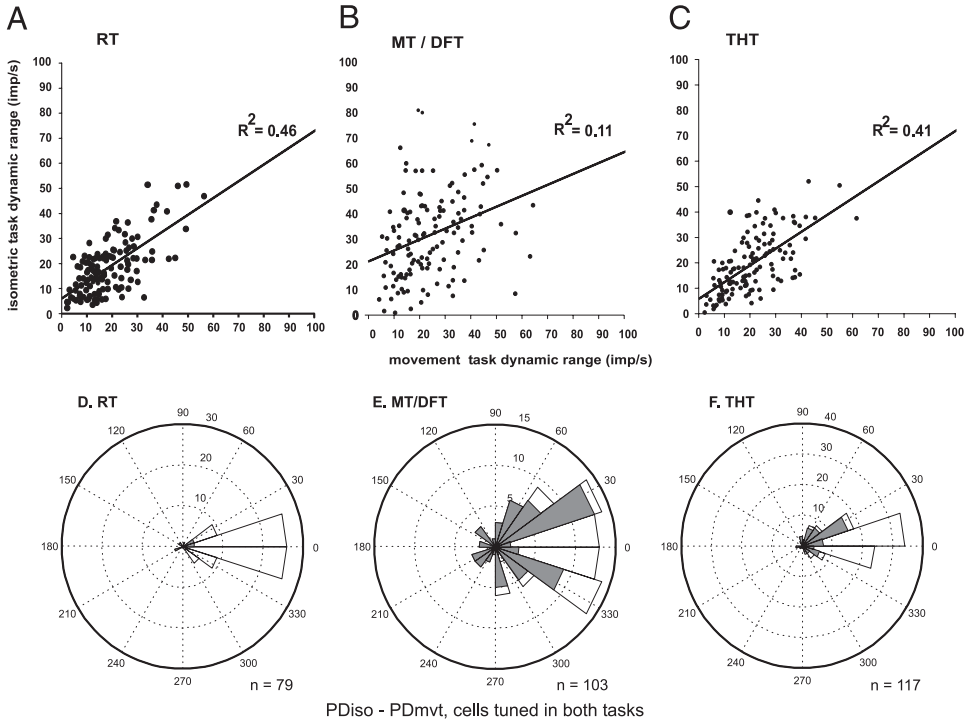

FIG. 5. *A–C*: scatter plots comparing the directional dynamic range of neuronal activity in the isometric vs. movement task during reaction time (RT) (*A*), MT/DFT (*B*), and THT (*C*) for all neurons that were directionally tuned in both tasks in those epochs. Solid line denotes the slope of the best-fit correlation for the dynamic ranges between the 2 tasks. Overall, there is a much weaker relation between the dynamic range in the 2 tasks during the MT/DFT epoch than in the RT and THT epochs. *D–F*: distributions of the differences in preferred direction (ΔPD) of single neurons in the isometric vs. movement task calculated by averaging the activity of neurons in each output direction during the RT (*D*), MT/DFT (*E*), and THT (*F*) epochs. Only neurons that were directionally tuned in both tasks in a given trial epoch are plotted. *n*, number of neurons that were directionally tuned in both tasks in a given epoch.

PD_{it} of single neurons often remained relatively constant throughout the trial in the isometric task (Fig. 6*A*). For instance, the neuron in Fig. 6*A* became directional about 100 ms before force onset with a PD_{it} near 195°, and retained that directional tuning with minor fluctuations for the rest of the trial (confidence interval of 6.7° for the range of windowed PD_{it} from 100 ms before to 1,000 ms after force onset). In contrast, the time course of instantaneous PD_{mt} was often very complex in the movement task (Fig. 6*B*). The neuron became directionally tuned shortly before force onset in the movement

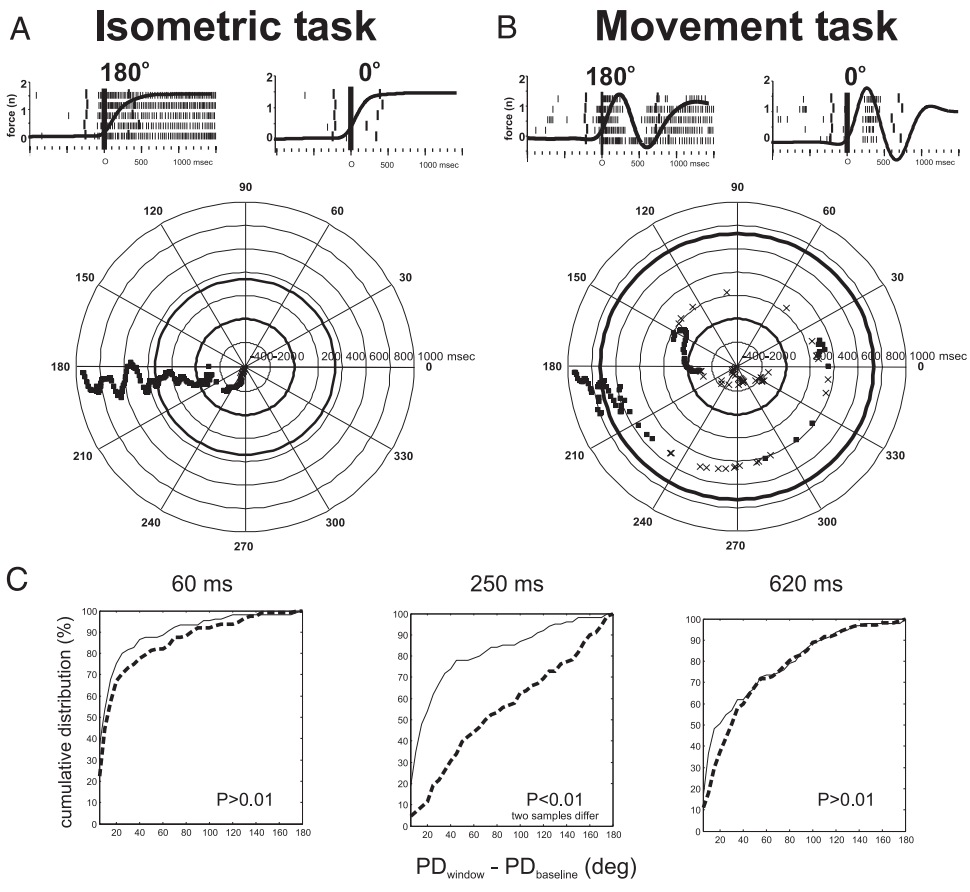

FIG. 6. *A* and *B*: rasters and direction–time trajectory of the moment-to-moment apparent preferred direction (PD) for the neuron shown in Fig. 4, in the isometric (*A*) and movement (*B*) tasks. Time progresses outward from the center to the perimeter of the plot. Preferred direction was calculated within a 50-ms time window that was incremented in 10-ms steps. Time windows during which the neuron was significantly directionally tuned are shown by a solid square. Time windows during which the neuron was not statistically directionally tuned are shown by an "×." Inner and outer thick circles denote force onset and movement/force ramp offset, respectively. *C*: cumulative distribution of the difference in PD for the whole neuronal sample at 3 points in time relative to force onset. PD_{window} refers to the PD of each neuron during a single 50-ms window beginning at a specific time in the trial (displayed above each panel). $PD_{baseline}$ refers to the PD during a single stationary 100-ms time window centered on force onset. Cumulative distributions are shown for the isometric (thin solid line) and movement (thick dashed line) tasks. A neuron had to be significantly directionally tuned at both moments in time to be included in the distribution for the corresponding task. A significant Kuiper's test ($P < 0.01$) indicated that the cumulative distributions of PD differences at a given moment in time relative to force onset were different between the 2 tasks.

task, with a windowed PD_{mt} near 195°. Shortly after force onset, the PD_{mt} began to change progressively in each successive window, to a momentary PD_{mt} of 5–20° near the peak of movement velocity at 300 ms after force onset (Fig. 6*B*), as the sliding window spanned the period corresponding to a pause in activity for movements to the left and a delayed burst for movements to the right. The PD_{mt} then rapidly rotated back to about 195° near the end of movement, although for much of the return rotation, the windowed activity was not significantly unimodally tuned (Fig. 6*B*).

To summarize the behavior of the entire population, a cumulative distribution was generated of the difference between a neuron's PD in a given 50-ms window at different times in a trial and its PD during a single fixed 100-ms "baseline" window spanning the time period ±50 ms relative to force onset in that task (Fig. 6*C*). A neuron had to be significantly directionally tuned both in the baseline window and in the 50-ms window to be included in the cumulative distribution for that particular time step. Figure 6*C* shows the cumulative distributions of PD differences for three different times in both tasks. In the 50-ms window, beginning 60 ms after force onset (Fig. 6*C*, *left*), 65% (movement task) and 75% (isometric task) of the neurons had a window PD that differed from their baseline PD by <20°, and 90% changed their PD by ≤60° in both tasks. This is not unexpected because that 50-ms window was adjacent to the baseline window. The cumulative distribution of windowed PD changes relative to baseline shifted systematically and gradually to larger values as time progressed in the trial in the isometric task (Fig. 6*C*), but 53% of the neurons were still within 20° of their baseline PD and 82% within 90° for the 50-ms window 620 ms after force onset (Fig. 6*C*, *right*). During the MT of the movement task, in contrast, neurons rapidly began to show a wide range of windowed PD differences from their baseline PD. Almost 45% of the cells had windowed PD changes of ≥90° 250 ms after force onset (Fig. 6*C*, *middle*; the distribution of PD changes in the movement task was nearly uniform at that time, deviating only slightly from a diagonal line). Near the end of the MT epoch, the windowed PD of many neurons was once again similar to that during the baseline window at force onset, and the distributions of PD changes were again very similar between the two tasks (Fig. 6*C*, *right*). Differences between tasks were significant at all time steps between 140 and 560 ms after to force onset ($D < 0.01$; Kuipers test; Batschelet 1981).

The preceding analysis assessed the stability of directional tuning of each neuron at different times in a trial within a given task. We next compared the directional tuning of neurons at the same relative point in time in the two tasks. Each neuron was subjected to two bootstrap tests (see METHODS). The first determined whether a neuron was significantly tuned within a task at each 50-ms time window. In the isometric task, the number of directionally tuned neurons increased rapidly during the RT epoch before force onset, and remained steady at between 74 and 81% of the neurons for the remainder of the trial (Fig. 7*A*). The incidence of directional tuning showed a very similar time course in the movement task (Fig. 7*A*).

We then calculated the difference in PD between the tasks for a given time window (ΔPDt). For this analysis, a neuron had to be directionally tuned in the same time window in both tasks. From 400 to 200 ms before force onset, the few neurons that happened to be significantly directionally tuned in both tasks showed nearly random ΔPD_t (Fig. 7*B*, mean ΔPD_t near 90°). This early part of the graph reflected the random nature of windowed tonic activity before and shortly after the appearance of the targets. As the sliding window began to encroach on the onset of the task-related response of each neuron, more neurons became directionally tuned in both tasks (Fig. 7*A*), and the mean ΔPD_t decreased rapidly, so that during the period

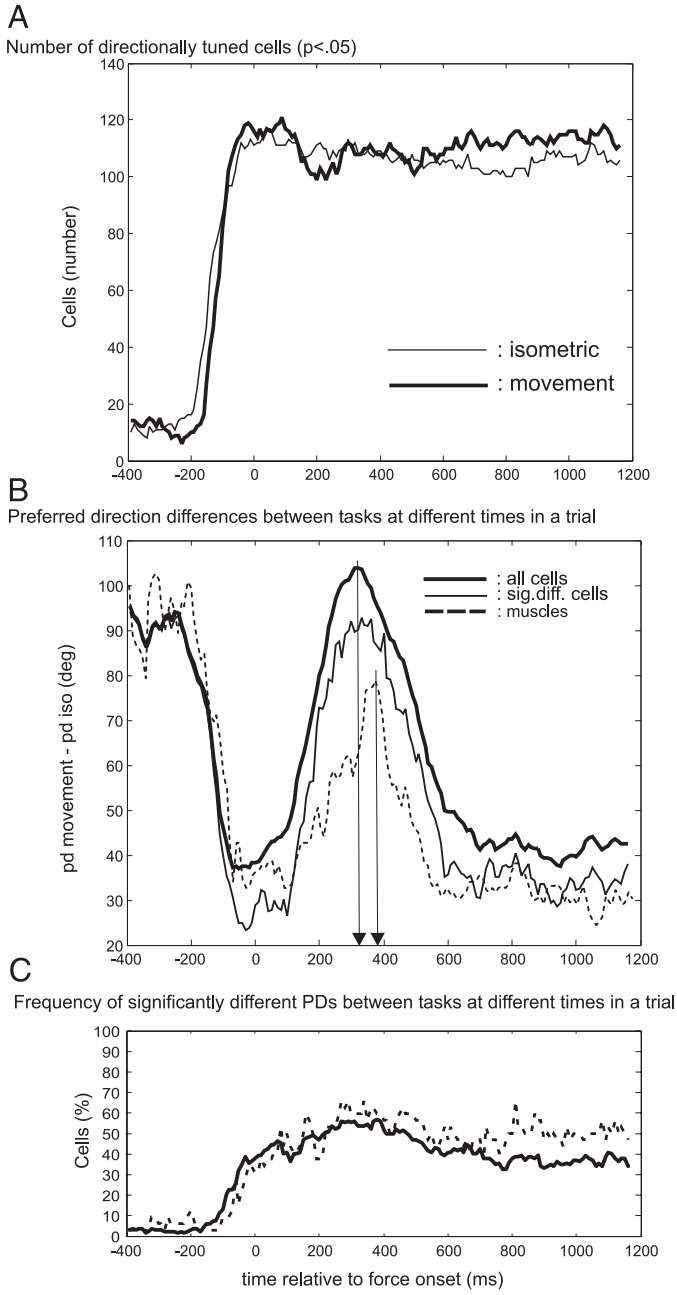

FIG. 7. *A*: number of directionally tuned neurons during a 50-ms window at different times in the movement (thick line) and isometric (thin line) tasks. *B*: mean difference in PD between the isometric and movement tasks for neurons that are directionally tuned in both tasks at a given time window (thick line), for neurons with a significantly different PD between tasks (bootstrap test; thin line), and for muscles with a significantly different PD between tasks (dashed line), over the time of a trial. *Time 0* represents the time of force onset. Vertical arrows denote the time of the peak difference in PDs between the 2 tasks for cells and muscles. *C*: percentage of neurons (solid line) and muscles (dashed line) having significantly different PDs between tasks over time.

±100 ms relative to force onset in each task, the directional tuning of the single neurons was very similar between tasks (Fig. 7*B*). The mean ΔPD_t then began to rise rapidly, peaking at 93° about 320 ms after force onset, and then declined again, returning to low values for the remainder of the trial. Unlike the results from 400 to 200 ms before force onset, these large differences in PD reflected the strong task-related responses of many task-related neurons (see Fig. 7, *A* and *C*). A corresponding analysis on muscle activity showed a similar pattern, shifted to slightly later times. A second bootstrapping procedure tested whether the change in directional tuning between tasks was significant for each single neuron at each time step (Fig. 7*C*). The incidence of significant ΔPD_t began to rise about 180 ms before force onset, peaked at 50–58% between 200 and 400 ms after force onset, and decreased to a fairly steady value around 35% beginning 700 ms after force onset (Fig. 7*C*). The time course and mean magnitude of ΔPD_t did not change substantially when only those neurons having a significant ΔPD_t between the two tasks at a given time step were used (Fig. 7*B*).

The MT epoch was about twice as long as the DFT epoch (Figs. 2 and 3), so the peak of the ΔPD_t distribution from 200 to 400 ms after force onset occurred in the middle of the MT but near the end of DFT as the monkeys were about to begin a period of static isometric force. However, the large ΔPD_t values were not an artifact of comparison of disparate functional phases in the two tasks. The trend began 100 ms after force onset, early in both the MT and DFT. The instantaneous PD_{it} remained fairly stable at all times during DFT and THT of the isometric task (Fig. 6). Finally, equally large ΔPD_t values were obtained when we compared the data in the time window from 250 to 300 ms after force onset in the movement task to the data in the middle of the DFT period of the isometric task from 150 to 200 ms after force onset (data not shown).

Population activity

Population histograms were generated by aligning the activity of all neurons that were directionally tuned in a given trial epoch of a task to their PD in that epoch (Fig. 8).

The mean population response of the neurons that were directionally tuned in the RT epoch of the isometric task (Fig. 8*A*, thick red line) showed an abrupt increase that began about 150 ms before force onset, peaked just before force onset, and then declined to a stable tonic rate at about the time the force output stabilized at the target force level (Fig. 8*A*, thin red line). The initial overshoot of population activity was not paralleled by an overshoot of force output. In the opposite force direction, the population activity decreased abruptly before force onset and remained at that level for the rest of the trial.

The population response for neurons that were directionally tuned in the RT epoch of the movement task showed a triphasic time course like that seen in single neurons (Fig. 8*A*, thick black line). An initial phasic burst at the PD began about 150 ms before force onset, peaked at force onset, and then began to decline rapidly. Activity reached a momentary minimum between 300 and 400 ms after force onset, followed by a second burst that peaked about 650 ms after force onset, and then a sustained tonic discharge for the rest of the trial. In the opposite direction, population activity showed an initial brief decrease before force onset, followed by a brisk burst of activity peaking

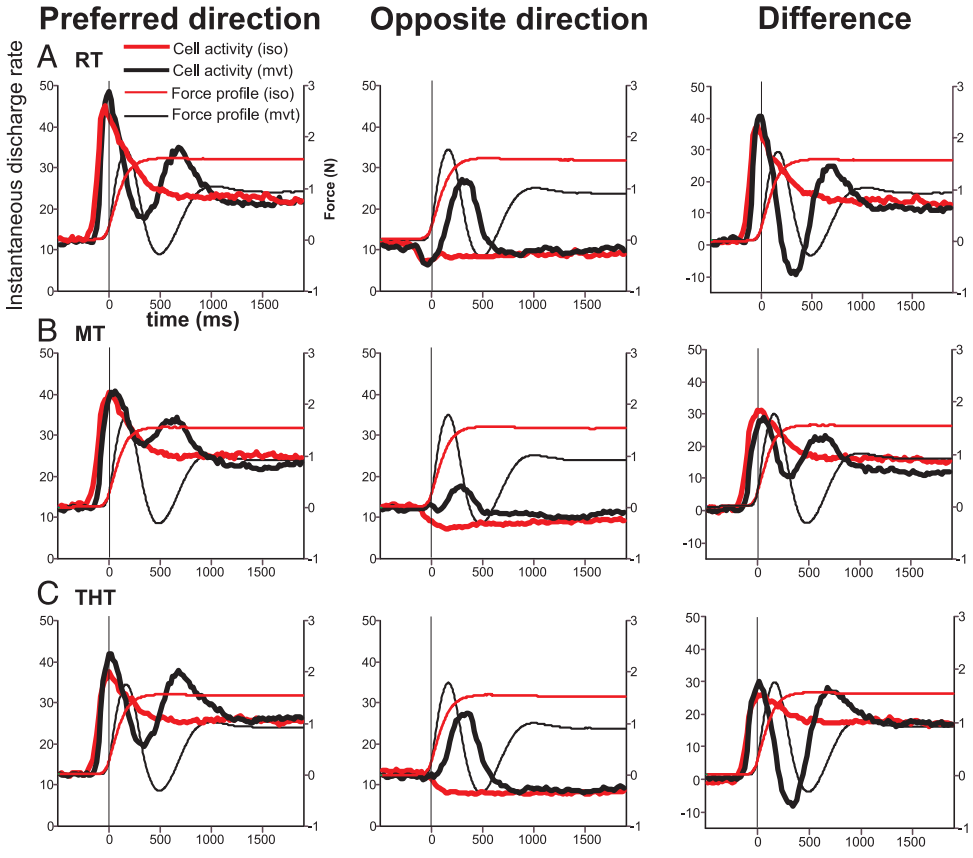

FIG. 8. Mean population histograms of the task-related activity of neurons that were directionally tuned in a given epoch of each trial, for their preferred output direction (*left column*) and opposite output direction (*middle column*) in the isometric (thick red line) and movement (thick black line) tasks. All data were aligned to force onset (*time 0*) in both tasks. Mean temporal force profiles at the hand are shown for the corresponding output directions in the isometric (thin red line) and movement (thin black line) tasks. *Right column*: population response-difference histograms calculated from the difference in mean population activity between the preferred and opposite output directions (*left* and *middle columns*, respectively) in the isometric (thick red line) and movement tasks (thick black line). Mean temporal force profiles at the hand averaged across both directions of output are also shown for the isometric (thin red line) and movement (thin black line) tasks.

300–400 ms after force onset, and then a low tonic discharge for the rest of the trial. The major components of the population responses led the corresponding components of the force profiles (Fig. 8*A*, thin black line) by about 150 ms.

The population histograms for the neurons that were directionally tuned during the THT epoch (Fig. 8*C*) were similar to those using the RT tuning. The most notable differences were that the initial phasic response at the PD was slightly weaker in both tasks and late tonic activity a little stronger compared with RT-aligned data, and that the suppression in the opposite direction is not evident before force onset. These response differences reflect differences in directional tuning at different times in the task (Fig. 6*C*; Crammond and Kalaska 1996, 2000).

The population histograms of activity aligned to the PD from the MT of the movement task showed a marked reduction in the depth of the transient decrease in activity during movement in the PD and in the amplitude of the delayed burst in the opposite direction. These changes resulted from the tendency for the calculated PD during the MT epoch to be biased toward the direction of movements in which the delayed burst occurred.

The population activity in the two tasks reflected to a first approximation the time course of measured force outputs. One discrepancy was the large initial activity overshoot at the PD of the isometric task. A corresponding overshoot may exist in the movement task, but was obscured by its complex temporal profile. An overshoot was evident, however, after the transient response suppression at the PD. Furthermore, the static force output at the hand was about 0.5 N greater during THT in the isometric task than in the movement task (Fig. 8, thin lines). However, the population activity converged on similar discharge levels in both tasks (Fig. 8, thick lines).

The population response profiles showed a gradual evolution across different directions of motor output in each task (Fig. 9) like that seen for single muscles (Figs. 2 and 4). The response profiles seen ±45° relative to each neuron's PD were similar to that at the PD in both tasks. Responses in the orthogonal directions were clearly transitional, and response profiles that were essentially reciprocal to that at the PD were seen for outputs ±135 and 180° away from the PD.

Activity in Figs. 8 and 9 was aligned arbitrarily at the PD of each neuron, to capture the mean direction-related changes in the time course of population activity. However, any given direction of motor output will be near the PD of some neurons and nearly opposite to the PD of others. This can be simulated by subtracting the population histogram for outputs opposite to the PD from the histogram at the PD (Fig. 8). The resulting difference histograms in the movement task show a strong initial response, followed by a net decrease in activity below baseline from 300 to 400 ms after force onset, and then a second increase in activity above baseline for the rest of the trial. The difference histograms show clearly how the time course of neuronal activity paralleled and led in time the profile of measured output forces. They also suggest that the transient changes in directional tuning in single neurons in the movement task were sufficiently consistent to produce a transient reversal of the net population-level directional signal during movement.

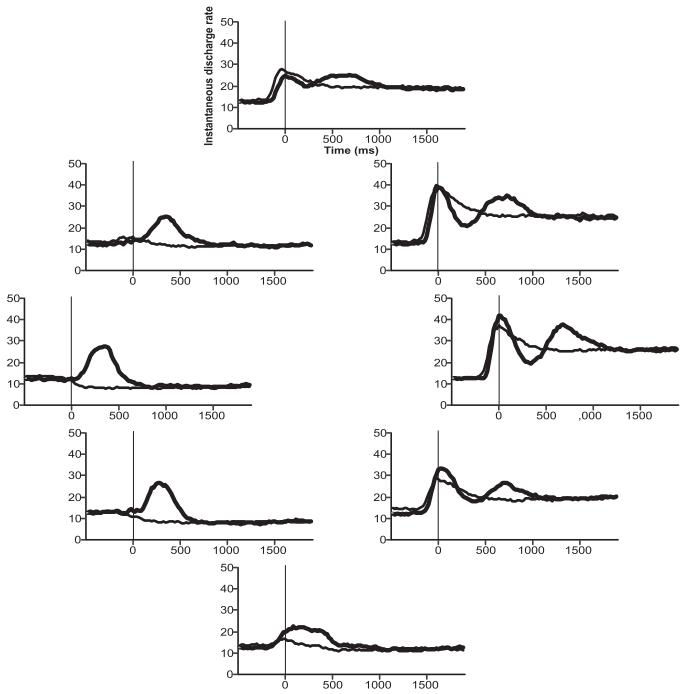

FIG. 9. Evolution of the mean population response as a function of output direction relative to the PD of each cell in the movement (thick line) and isometric (thin line) tasks. All data were aligned to the time of force onset (*time 0*) and the PD of each neuron for arm movement or isometric force was arbitrarily rotated to the *right*. Histograms were generated for those neurons that were directionally tuned during THT, using the PD from that epoch. Similar gradual changes in the response profile across directions were obtained when histograms were generated for neurons aligned to their preferred direction in the RT and MT/DFT epochs, although the triphasic response profile is not as pronounced when aligned to the PD during the MT epoch (cf. Fig. 8; data not shown).

Population vector analysis

This prediction was tested by a vectorial reconstruction of activity within a time sequence of nonoverlapping 20-ms windows, which provides a rich description of the moment-to-moment directional bias of population activity in different tasks (Georgopoulos et al. 1988, 1992; Moran and Schwartz 1999b; Schwartz 1993, 1994; Wise et al. 1996).

Figure 10 shows the results from the entire sample of 132 neurons for 0 and 180° motor outputs. In the isometric task, the direction of the change in output forces relative to the force

FIG. 10. Population-vector representation of the moment-to-moment net directional signal generated by the entire sample of 132 M1 neurons (solid circles) during the isometric force (*A*) and movement tasks (*B*). Vectors are shown for the rightward (0°) and leftward (180°) directions in each task. Time progresses downward. Each vector represents the direction and magnitude of the net population signal generated by the full sample of neurons during a 20-ms time window that was advanced in nonoverlapping 20-ms steps. Strength of the contribution made by each neuron to each population vector was proportional to the change in activity at a given time and direction of motor output relative to its mean discharge rate during CHT. PD assigned to each neuron was calculated from the averaged activity of the neuron during the entire THT epoch. Mean change in force output vector relative to the bias force during the CHT is also shown at each 20-ms interval (open circles). Direction–time trajectory of neuronal population-vector direction (filled circles) and force output vector direction (open circles) are shown in polar-plot format below each of the corresponding vector plots.

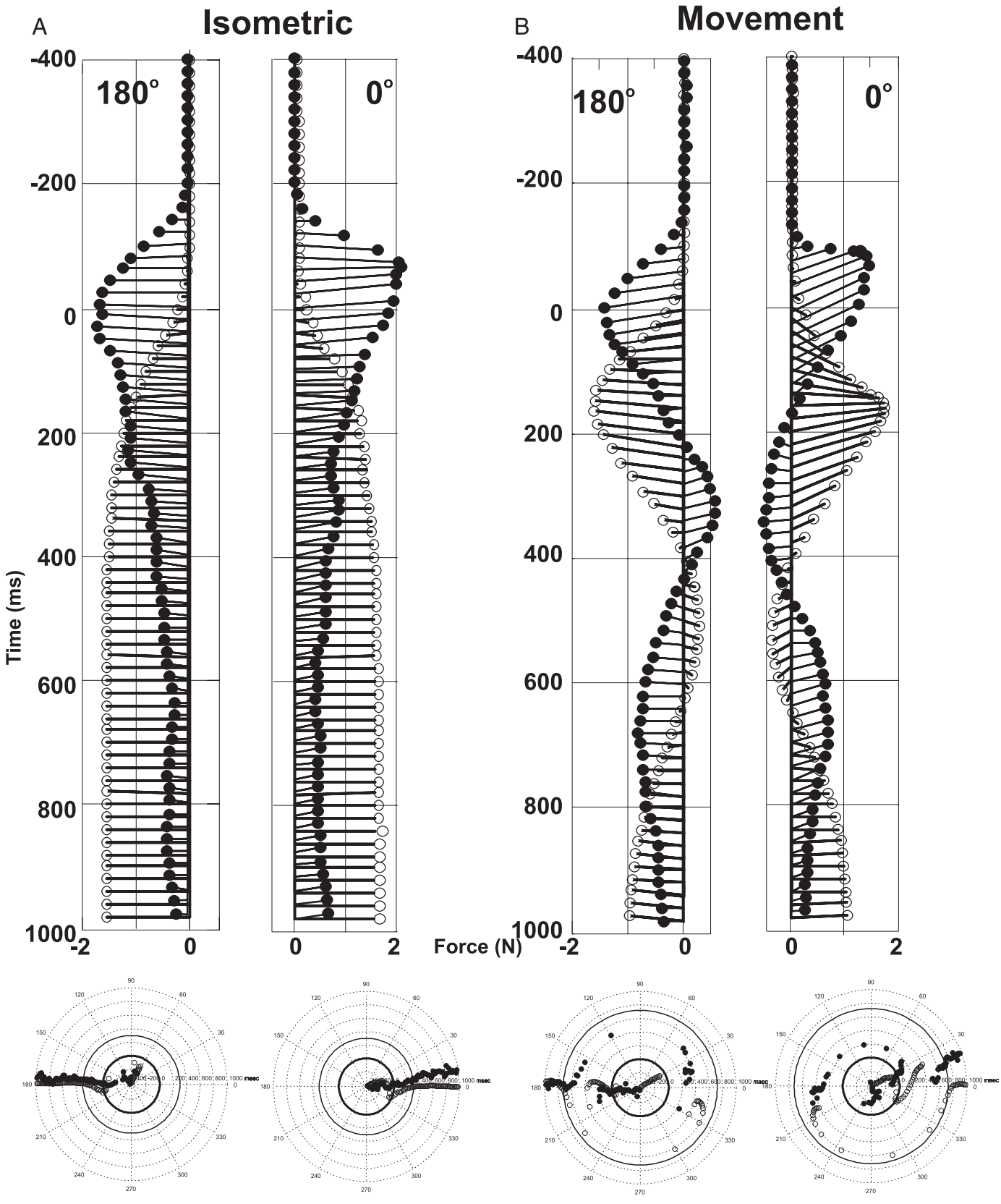

offset bias during CHT pointed in the target direction (Fig. 10*A*, open circles). The length of the force vectors began to increase at force onset, reached a peak of about 1.5 N within 400 ms after force onset, and remained at that length throughout THT. The 20-ms population vectors likewise varied systematically with force direction (Fig. 10*A*, filled circles). They began to grow in the direction of force output 160–140 ms before force onset and showed little variation in direction throughout the trial. The length of the population vectors grew rapidly before force onset and peaked near force onset, then decreased to a shorter length (cf. Fig. 8, cell histograms).

The pattern of force and neuronal population vectors changed in the movement task. The change-in-force vectors (Fig. 10*B*, open circles) initially pointed in the direction of the peripheral target and increased in length for about 180 ms after force onset. They then began to decrease in length and eventually reversed direction at about 400 ms after force onset. This reflected the deceleration forces required to brake the motion of the pendulum as it approached the peripheral targets. The force vectors then reversed direction again back toward the target direction about 600 ms after force onset, and stayed at a steady direction and force level during THT.

The neural population vectors in the movement task displayed similar patterns (Fig. 10*B*, filled circles). There was an initial increase in vector length in a direction corresponding fairly closely to that of the target, beginning about 160–140 ms before force onset and peaking in length at about the time of force onset. The population vectors then began to decrease in length and reversed direction at about 200 ms after force onset. The vectors later reversed direction again, pointing toward the targets for the remainder of the trial.

Figure 10 was generated using the PD of neurons during the THT epoch. Repetition using the PDs from the RT epoch did not substantially alter the basic findings (not shown).

Figures 11 and 12 display the time course of the direction of the force and population vectors for the other output directions in a polar-plot format (cf. Fig. 10, *bottom*). In the isometric task, the force vectors pointed in the target directions from the time of force onset to the end of the trial (Fig. 11). The population vectors also maintained a fairly constant direction from the onset of force to the end of the trial. There was, however, a systematic bias in the direction of the population vectors toward the lateral (0–180°) directions, especially for the diagonal force output directions, that was sustained during the final static-force period of THT (Fig. 11).

In the movement task (Fig. 12), the change in measured output forces started off in the intended direction of movement, then rapidly reversed to point in the opposite direction during MT, and then returned to the intended direction of movement for the rest of the trial. The direction–time trajectory of the neuronal population vectors showed similar trends for most movement directions, in particular 225, 270, and 315° (Fig. 12). For 45 and 135°, large transient deviations of population vectors from the direction of movement were also seen but they did not result in a complete reversal of vector orientation (Fig. 12). Finally, the direction of the population vectors remained fairly constant after force onset for 90° movements, even though the measured output forces at the hand reversed direction during movement (Fig. 12). For some directions, the force and population vectors rotated in opposite directions during the reversals.

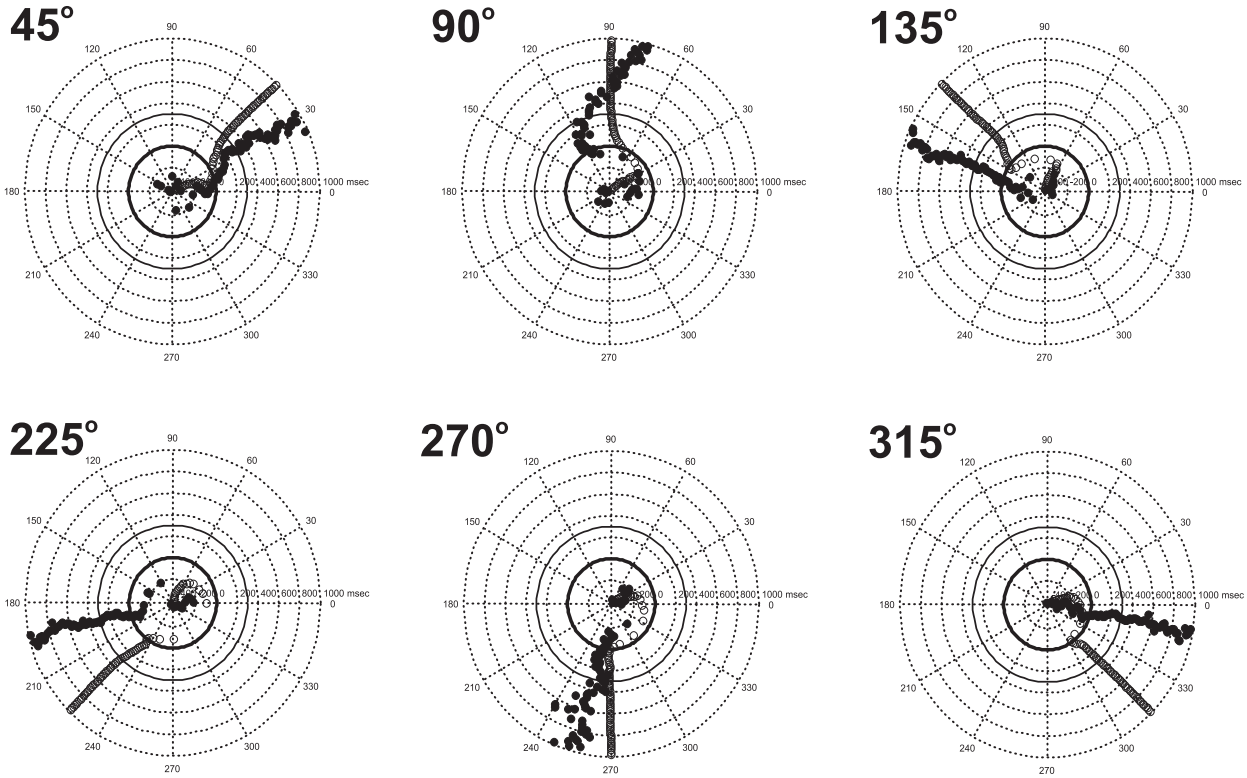

FIG. 11. Direction–time trajectories of neuronal population vectors (solid circles) and mean force output vectors (open circles) for the 45, 90, 135, 225, 270, and 315° force directions in the isometric task. All 132 neurons were used. Same format as the polar plots in Fig. 10.

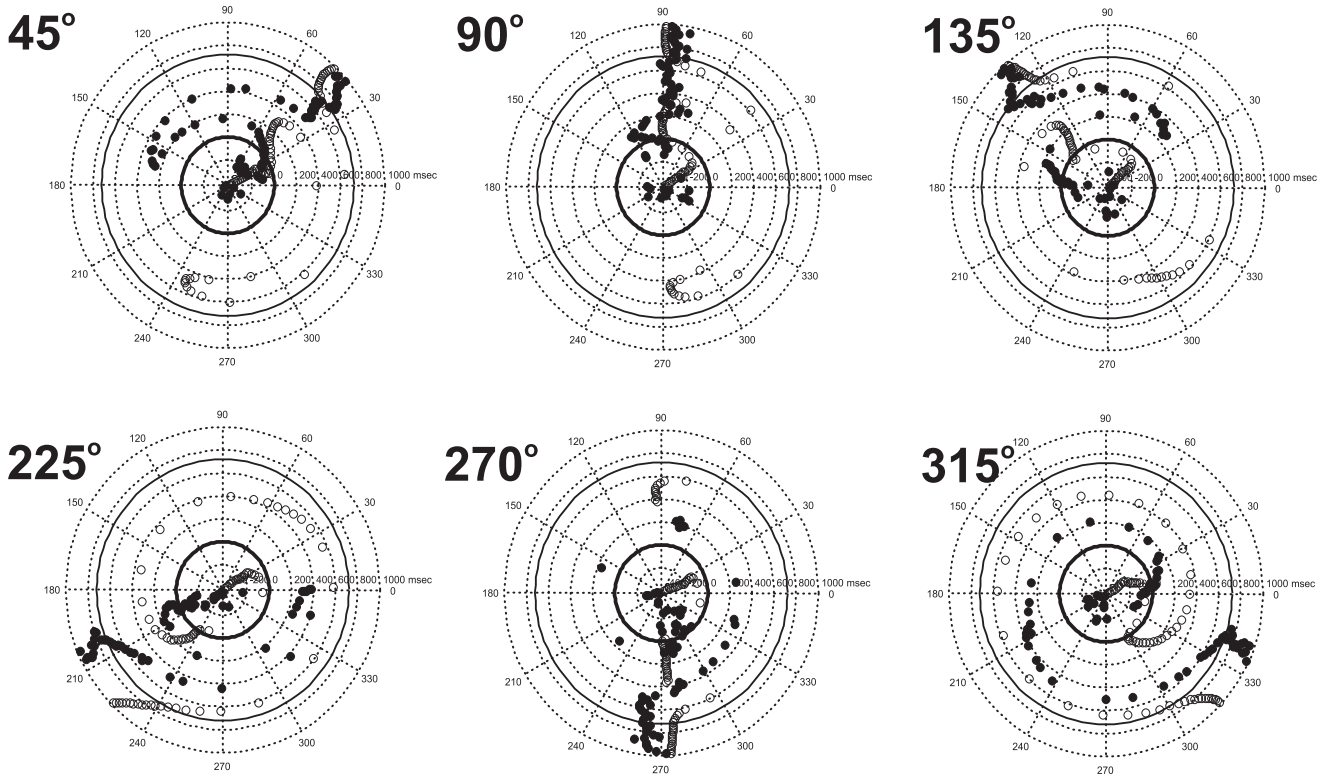

FIG. 12. Direction–time trajectories of neuronal population vectors (solid circles) and mean force output vectors (open circles) for the 45, 90, 135, 225, 270, and 315° movement directions in the movement task. All 132 neurons were used. Same format as in Fig. 11.

Figures 11 and 12 show only the directions of the vectors but ignore their length. This information is provided in a direction-magnitude polar plot (Fig. 13). The force trajectories grew monotonically in the desired direction in the isometric task. In the movement task, in contrast, they grew rapidly in magnitude in the desired direction, then abruptly decreased in length and changed direction, before swinging back in the direction of movement. The magnitudes of the force vectors were uniform across all directions of motor output in both tasks.

In contrast, the neuronal population vectors in the isometric task grew rapidly in length but then decreased significantly. The direction–magnitude trajectories of the population vectors were more complicated in the movement task, but in most cases reflected the corresponding complexity of the measured output forces at the hand. The bias in vector directions toward the 0–180° axis seen in the direction–time trajectories (Figs. 11 and 12) is also evident in the direction–magnitude trajectories (Fig. 13). There was also a large nonuniformity in the magnitude of the population vectors in both tasks. They were much longer for movements along the lateral (0–180°) axis than the orthogonal (90–270°) axis, unlike the directional uniformity of measured motions and forces in those tasks.

Finally, studies have shown a good correspondence between the spatial kinematics of hand motions and a "neural trajectory" constructed by linking the momentary population vectors tip to tail. Figure 14 illustrates the neural trajectories constructed from the 20-ms population vectors of our data in both tasks, as well as the hand-displacement trajectories and force trajectories made by linking the 20-ms force vectors. In the isometric task, there was no hand displacement, by definition, and forces increased monotonically in each output direction. Neural trajectories likewise grew monotonically with time, but with a bias in direction and magnitude toward the lateral axis. In the movement task, the hand moved smoothly toward each target. In contrast, the force trajectories showed the transient reversals of measured output forces to decelerate the pendulum. The neural trajectories also showed striking reversals for all directions except 90°.

DISCUSSION

Summary of principal findings

This study showed that many M1 neurons were strongly activated in both whole-arm isometric-force and movement tasks. There was no compelling evidence of selective recruitment of neurons in specific dynamical environments. The second major finding was that many M1 neurons showed striking changes in the time course and apparent momentary directionality of their activity between the tasks that paralleled the differences in time course of output dynamics in the tasks. The isometric task required monotonic ramps of output forces aimed continuously in the target direction, whereas the movement task required an initial accelerative force applied to the heavy pendulum handle followed by a transient reversal of the direction of applied forces to decelerate the pendulum. The directional tuning of single-neuron activity was generally similar in the two tasks during the behavioral reaction time before overt motor output and during the final static-hold period, but often showed substantial differences in apparent directionality during the dynamic motor-output epoch itself. Population-vector signals showed similar task-dependent effects. The direction of the population signal remained relatively constant during the dynamic force ramps of the isometric task. In the

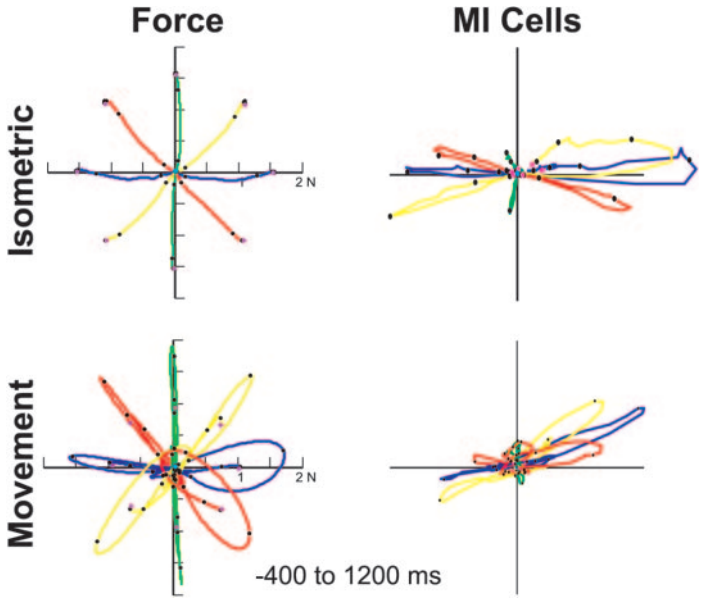

FIG. 13. Direction–magnitude trajectories of force output vectors and neuronal population vectors in the 2 tasks. Trajectory for each output direction was drawn by plotting all the vectors for that output direction with their tails at the center of the plot and joining the tips of the sequence of individual vectors by a line. Vectors themselves are not shown. Trajectories begin 400 ms before force onset and continue to 1,200 ms after force onset. Black dots are drawn on the trajectories at 200-ms intervals.

movement task, in contrast, population activity captured the transient reversal of the direction of hand-centered output forces when they were momentarily dissociated from the direction of motion during the deceleration phase of the movements. The M1 signals led the peripheral outputs by about 150 ms, thereby representing a potential feedforward control signal reflecting predictable differences in output dynamics between the two tasks.

A third major finding was a directional anisotropy in the neuronal population output signals. The magnitude of the signals was significantly greater for lateral (0–180°) directions of motor output than for orthogonal (90–270°) outputs, and the directionality of the signals for diagonal motor outputs was biased toward the 0–180° axis. These anisotropies were more prominent in the isometric task than in the movement task. Finally, the transient reversal of output signals during arm movements was pronounced for lateral directions but was essentially absent for movements in the orthogonal axis away from the body (90°).

Task dynamics and muscle activity

A critical manipulation in this study was the inertial load imposed by the pendulum. The extra weights that were added to the force transducer assembly and the maximum allowable movement time of 750 ms were set empirically to ensure that the peak initial accelerative force during MT and the final static horizontal forces during THT to hold the pendulum over the targets against gravity were both similar in scale to the final

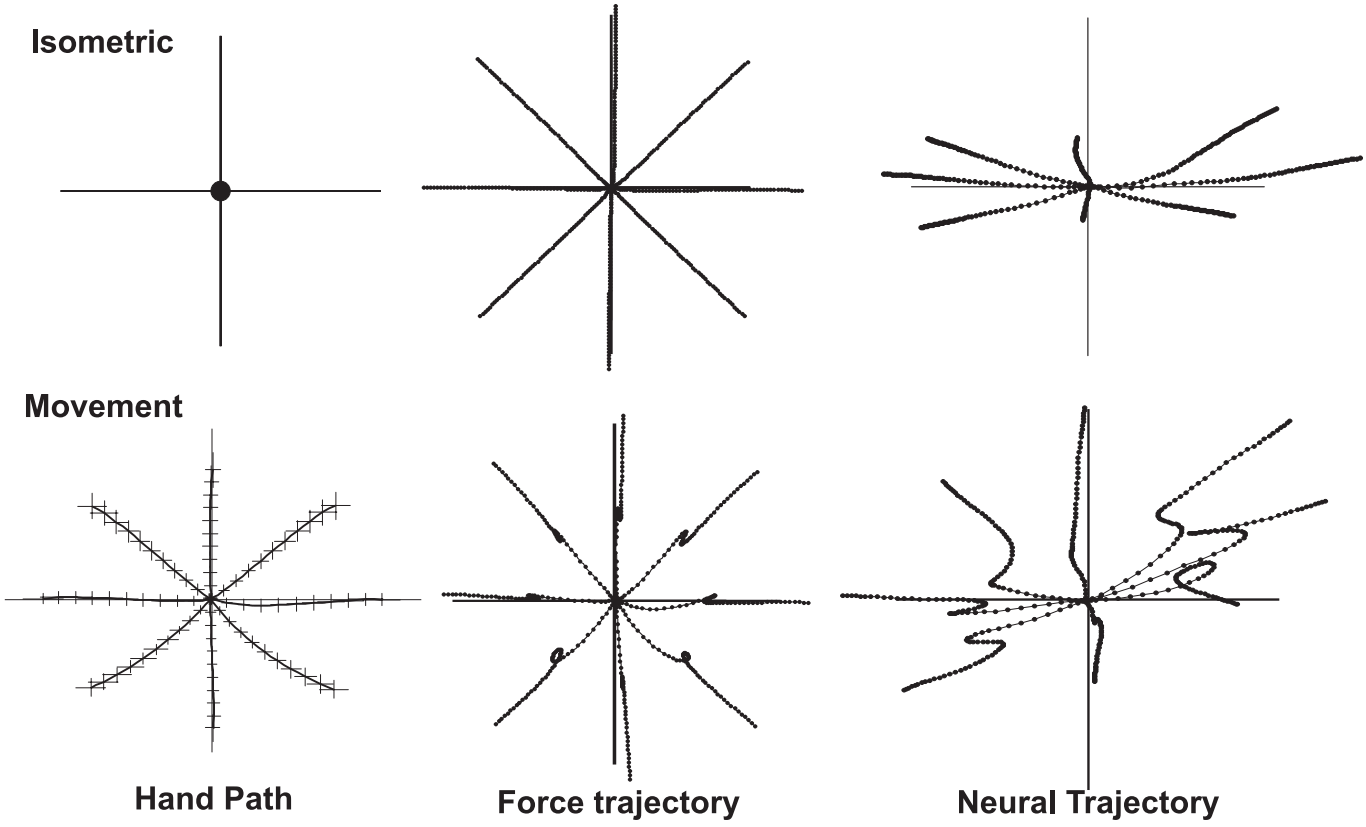

FIG. 14. Comparison of output kinematics, kinetics, and neuronal population activity in the 2 tasks. Figures show the mean hand paths (*left*), force trajectories (*middle*), and neural trajectories (*right*). Force and neural trajectories were generated by linking the sequences of 20-ms output force vectors or neural population vectors tip-to-tail, for each direction of force or movement output.

static isometric forces. The monkeys had to move the pendulum rapidly and then decelerate it to hold it over a small target, while also controlling the vertical forces exerted out of the plane of motion. This altered the time course of output forces at the hand between the isometric and movement tasks, and caused a transient dissociation of the directionality of output forces and motions during the movement. Output forces were measured only at the hand and no direct measure of active and passive internal forces was available. However, muscle activity reflects all of those factors and so provides an excellent global measure of the impact of task dynamics on motor output.

The load caused a striking change in muscle activity, from directionally tuned ramps in the isometric task to the classic triphasic pattern in the movement task, characterized by an agonist burst followed by a brief pause in activity during movement in the agonist direction of each muscle, and a braking pulse of activity during movement in the opposite direction (Brown and Cooke 1990; Cooke and Brown 1990; Corcos et al. 1989; Flanders 1991; Hoffman and Strick 1999; Wadman et al. 1980). The triphasic EMG has been extensively studied. It arises during single- and multijoint movements and is seen both in muscles acting across moving joints and acting across stationary joints that must be stabilized during movement of other parts of the limb (Brown and Cooke 1990; Cooke and Brown 1990; Corcos et al. 1989; Flanders 1991; Gribble and Ostry 1998, 1999; Hoffman and Strick 1999; Koshland et al. 2000; Wadman et al. 1980). It can even arise during very rapid (<120 ms) targeted isometric-force pulses, possibly to compensate for the low-pass filter properties of the musculoskeletal plant (Ghez and Gordon 1987). Although the magnitude and timing of each triphasic response component are indirectly determined by the kinematics of movement, including direction, speed, acceleration, distance, and duration (Brown and Cooke 1990; Buneo et al. 1994; Cooke and Brown 1990; Corcos et al. 1989; Flanders 1991; Ghez and Martin 1982; Karst and Hasan 1991a,b; Wadman et al. 1980), they directly reflect movement dynamics, that is, the forces and torques needed to move each limb segment and to cope with external loads and the interaction torques that arise between limb segments during movement (Gribble and Ostry 1999; Gribble et al. 1998; Hollerbach and Flash 1982; Zajac and Gordon 1989).

The triphasic activity seen in proximal-arm muscles in this study likewise reflected the shoulder and elbow torques required to move the arm and the large handheld mass between targets and to compensate for the interaction torques that arose at those joints. The triphasic pattern was centered on the preferred movement axis of each muscle and showed a gradual transition between agonist and antagonist profiles for intervening movement directions (Flanders 1991; Hoffman and Strick 1999; Karst and Hasan 1991a,b; Wadman et al. 1980).

The origin of the triphasic EMG pattern is still not resolved. The consensus is that it is centrally programmed, but that sensory feedback is critical to adjust its timing and scaling, especially the braking pulse (Forget and Lamarre 1987; Hallett et al. 1975; Sainburg et al. 1995, 1999). However, controversy remains as to whether the response is explicitly encoded by descending supraspinal control signals or is indirectly evoked by descending modulation of the thresholds and gains of spinal reflex circuits (Feldman 1986; Fetz et al. 2000; Gribble et al. 1998; Loeb 1987; Ostry and Feldman 2003; Todorov 2000). We will return to this issue in later sections.

Relation of the present results to previous studies of motor cortex

Many studies have reported systematic relations between M1 activity and output forces or muscle activity during single-joint and whole-arm isometric-force tasks or movements against external loads (Ashe 1997; Cheney and Fetz 1980; Lemon and Mantel 1989). The present study is consistent with those findings. Most studies focused on neuronal correlates of static forces, whereas M1 correlates of dynamic forces have not been as thoroughly studied (Ashe 1997; Li et al. 2001; Smith et al. 1975). Few studies used inertial loads. Most previous studies sought scalar correlates with the magnitude of forces in one-dimensional tasks (Ashe 1997; Cheney and Fetz 1980), or with the direction (Georgopoulos et al. 1992; Li et al. 2001) or direction and magnitude (Taira et al. 1996) of 2D and 3D forces. This study used a different approach to assess the relation of M1 activity to task dynamics. It is the first study to our knowledge to directly compare the activity of M1 neurons in both a 2D isometric-force task and a 2D whole-arm movement task with an inertial load. The tasks differed in their intended kinematics (movement in one but not in the other) and required dynamics (inertial loads in one, monotonic force ramps in the other). The findings show that activity in the caudal part of M1 in the bank of the central sulcus is strongly modulated by differences in the temporal pattern of output forces between the tasks.

All previous studies in our lab used a very light pendulum. Nevertheless, neurons with triphasic responses were also seen in those studies, but less frequently than here. About 30% of the neurons in two studies (Crammond and Kalaska 1996; Kalaska et al. 1989) had "phasic–tonic" responses similar to the triphasic pattern seen in 61% of the neurons in this study. Significantly, the "phasic–tonic" neurons were also strongly modulated by the changes in task kinetics caused by constant external loads (Kalaska et al. 1989). The presence of M1 neurons displaying triphasic responses in those studies show that they do not discharge only when the system is confronted with large external inertial loads. In the earlier studies, their triphasic activity patterns likely reflected the output dynamics required to move the monkeys' arm and the lightweight pendulum. Moreover, the present study showed that not only do "triphasic" neurons discharge in an isometric-force task but that the temporal pattern of their activity changes in the absence of an inertial load.

The inertial load also distinguishes this study from free-arm motor tasks (Caminiti et al. 1990, 1991; Georgopoulos et al. 1988; Moran and Schwartz 1999a,b; Schwartz 1992, 1993, 1994; Schwartz and Moran 1999; Schwartz et al. 1988). Those studies reported correlations of M1 single-neuron and population activity with the overall direction and the moment-to-moment kinematics of hand motion during reaching movements and continuous figural-tracing motions of the arm. In contrast, the present study found a transient dissociation of the directionality of M1 activity and movement kinematics during arm movements in several directions.

One possible factor for the discrepancy in results is the region of cortex sampled in the different studies. Recordings in

this study were made in the caudal part of M1 in the bank of the central sulcus, where neuronal activity is strongly modulated by external loads (Kalaska et al. 1989). In contrast, much of the data in the other studies came from more rostral M1 on the exposed surface of the precentral gyrus. Both the incidence of neurons with triphasic responses during reaching and the sensitivity of neurons to loads and forces diminish with distance from the sulcus (Crammond and Kalaska 1996; Kalaska et al. 1989; Scott and Kalaska 1997; Werner et al. 1991). This may represent a rostrocaudal gradient in the functional role of M1 neurons, or in their somatotopic relationship with the motor periphery, or other factors. Nevertheless, the nature of the signal extracted from M1 will depend in part on the region sampled.

Another possible factor is that the kinetics of the free-arm tasks did not provide a sufficient dissociation between the direction of motions and forces. For instance, 3D reaching movements were often halted when a monkey's hand made contact with a button (Caminiti et al. 1990, 1991; Georgopoulos et al. 1988; Schwartz et al. 1988). In contrast, in the present study, the monkeys had to halt the motion of their arm and a heavy free-swinging pendulum over a target by applying a decelerating force on the pendulum. Movements were also not halted by striking a target in some other reaching studies (Moran and Schwartz 1999a,b; Schwartz 1992, 1993, 1994; Schwartz and Moran 1999), but in those studies the monkeys slid their finger across the surface of a touch screen and did not require active antagonist braking EMG pulses to halt movement (Moran and Schwartz 1999a,b).

Similarly, to change movement direction in continuously curved figural-tracing tasks, the Newtonian laws of motion require the motor system to apply a tangential accelerative force vector perpendicular to the normal forces causing the current direction of motion, whose magnitude depends on the speed and desired curvature of the hand path (for simplicity, we will ignore the fact that the direction of forces and motions are not always co-linear in multiarticular systems). The resultant summed output force vector will deviate from the current direction of motion. However, if the speeds or curvatures of the motions are not high enough, any M1 activity related to the direction of output dynamics will remain near the direction of motion at all times. In at least one such study, the EMG activity correlated well with direction and speed but not with normal or tangential acceleration (Moran and Schwartz 1999a,b; Schwartz and Moran 1999), indicating that the task conditions did not impose a large dissociation of the directionality of forces and motions. In contrast, in this task, the monkeys applied a braking force to the handle opposite to the direction of motion, providing the optimal conditions to observe a component of M1 activity that reflects the direction of output dynamics, dissociated from output kinematics. Even in the present task, if the movements had been slower or of smaller amplitude, the combined inertia of the arm and pendulum may not have required active braking, and the motions could have been halted by gravity and internal viscoelastic damping forces within the musculoskeletal plant as the arm pushed the pendulum away from the start position toward the targets.

Another potential factor is the control strategy used to perform the tasks. The highly practiced monkeys in this study made stereotyped point-to-point arm movements with very predictable dynamics. In such conditions, subjects rapidly learn to use predictive feedforward control of task dynamics (Gandolfo et al. 1996; Krouchev and Kalaska 2003; Lackner and DiZio 1994; Li et al. 2001; Sainburg et al. 1999; Shadmehr and Mussa-Ivaldi 1994; Thoroughman and Shadmehr 1999, 2000). The monkeys in this study made arm movements by precisely timed reciprocal activation of antagonist muscles, rather than by graded coactivation to minimize the perturbing effects of the load. M1 activity changed between the tasks to parallel the differences in task dynamics and consistently led the output by 100–150 ms. This evidence suggests that these highly skilled monkeys performed the tasks at least in part by predictive feedforward control of dynamics, and that this control mode was strongly expressed in caudal M1.

In contrast, figural-tracing studies, especially those with random target motions (Paninski et al. 2004a,b), likely put a premium on feedback control of hand paths and provided less than optimal conditions for an extensive degree of predictive control of output dynamics. Such conditions may also have encouraged a significant degree of graded muscle coactivation to critically dampen and stabilize the limb to facilitate control of hand motion. Most published descriptions are not sufficiently detailed to assess the degree to which the monkeys used reciprocal control or graded coactivation of muscle activity in those tasks. Nevertheless, the difference in results may reflect the degree to which task performance can be facilitated by predictive control of output dynamics.

A related potential factor is a context-dependent change in the prominence of different classes of output parameters in M1 in different tasks. Neuronal operations in M1 may not be invariant across tasks. On the contrary, it is well established that M1 activity can be altered by the nature of the task, such as when generating precisely controlled forces rather than brusk agitated actions (Cheney and Fetz 1980), during independent or precision-pinch actions of the digits rather than power grips (Buys et al. 1986; Hepp-Reymond et al. 1999; Lemon and Mantel 1989; Maier et al. 1993; Muir and Lemon 1983; Smith et al. 1975), during precise biting rather than rhythmical chewing (Hoffman and Luschei 1980), and during modification of the locomotor step cycle to avoid obstacles (Drew 1993). Similarly, M1 activity correlated with the total force output during static isometric force generation (Georgopoulos et al. 1992; Taira et al. 1996), but was better related to the change in force output during a dynamic force-pulse period of the same task (Georgopoulos et al. 1992). None of these cases can be explained by a fixed relationship between neuronal activity and output kinematics, kinetics, or muscle activity across conditions.

The present tasks placed a premium on the control of hand-centered output dynamics both in the horizontal plane and perpendicular to that plane, to move the cursor into the targets in both tasks. This may have led to an enhanced prominence of kinetics parameters in M1 in the present study, and in other reaching tasks with external loads (Gribble and Scott 2002; Kalaska et al. 1989; Li et al. 2001; Padoa-Schioppa et al. 2002, 2003). In contrast, the figural-tracing tasks required close control of the spatial kinematics of hand motions that may have led to an enhanced representation of kinematics parameters in M1, independent of any difference in causal dynamics across tasks. This is speculative, but the principle of context dependency of M1 activity has experimental support. It is thus possible that the control of the dynamics of stereotypical

unimpeded or unperturbed movements may be accomplished to a significant degree by subcortical circuits and is correspondingly underrepresented in M1 (Drew 1993). This is also the perspective of position-control models, although for different reasons.

Furthermore, it is increasingly evident that motor cortex circuitry is adaptive and is implicated in the acquisition of motor skills (Classen et al. 1998; Kargo and Nitz 2003, 2004; Li et al. 2001; Nudo et al. 1996; Paz and Vaadia 2003, 2004; Rioult-Pedotti et al. 1998). Context-dependent changes in the nature of the M1 motor representation itself, whether resulting from differences in task demands or from skill acquisition, may be another manifestation of the adaptive capacity of M1 circuitry. It is striking that neuronal correlates of output kinetics are routinely found in M1 of animals trained to perform tasks that directly manipulate those parameters (e.g., Gribble and Scott 2002; Kalaska et al. 1989; Li et al. 2001; present study), whereas representations of task kinematics are prominent (e.g., Georgopoulos et al. 1988; Moran and Schwartz 1999a,b; Paninski et al. 2004a,b; Schwartz 1992, 1993, 1994) and post hoc analyses (e.g., Ashe and Georgopoulos 1994; Moran and Schwartz 1999a,b; Schwartz and Moran 1999) often find relatively little evidence of kinetics representations, such as correlations with acceleration, in M1 of animals trained to perform unperturbed free-arm movements. Independent of the other factors already discussed, it may be necessary to reassess the degree to which the representation of output parameters in M1 may adapt to the nature and control demands of different task conditions, and thus influence the degree to which the motor representation seen in M1 in a given experiment is related to higher- versus lower-order task parameters.

Some studies have reported large and seemingly random changes in single-neuron activity during motor learning (Carmena et al. 2003; Kargo and Nitz 2003, 2004; Taylor et al. 2002). Those findings imply that each M1 neuron is a nearly unconstrained degree of freedom whose response properties after learning are empirically shaped by the unique history of changes in M1 circuitry during the learning process. We have no observations of neuronal activity during skill acquisition because recordings were made after lengthy training. However, indirect evidence does not support unrestricted plasticity of M1 responses in our tasks. Virtually all neurons tested were active in both tasks. The directionality and dynamic range of responses were generally similar during the RT and THT epochs of both tasks, and response changes across tasks during MT/DFT paralleled the changes in task dynamics. These findings suggest that single neurons in caudal M1 had a consistent role coupled to the directionality of motor output in both tasks, and that their responses were adapted in disciplined fashion to different dynamical conditions during learning.

Conceptual issues and limits of interpretation

COMPARISON OF RESULTS FROM THE TWO TASKS. A number of factors will confound a rigorous quantitative parametric comparison of the relation of M1 activity to task dynamics across task conditions in this study. The isometric task required simple force ramps in a fixed arm posture. The movement task, in contrast, required motor commands to move and hold the arm in different postures, to cope with the resulting internal and external dynamic forces during movement, and to push the pendulum up a static force gradient generated by gravitational forces on the pendulum. Output forces were measured only at the hand and internal active and passive viscoelastic forces were not measured. The ranges of measured output forces were very similar but not identical in the two tasks. The dynamic-force epoch was longer in movement trials than in isometric trials. We could have required the monkeys to make slower isometric ramps but that artificial constraint may have unwittingly introduced other modulating influences on cell activity independent of force outputs. Instead, we chose to let the monkeys perform at a pace set by their level of motor skill in both tasks, within the maximum-time limits. The peripheral feedback generated during the two tasks undoubtedly differed. These and other factors would make it difficult to interpret the significance of any quantitative differences in the relation of M1 activity to static and dynamic forces and their derivatives between tasks. As discussed elsewhere, however, not one of these factors on its own can account for the major finding of this study that caudal M1 cells generate a predictive feedforward signal that reflects the principal difference in task dynamics between the two tasks, that is, the transient reversal of direction of dynamic output forces during the deceleration phase of the movement task.

INVERSE TRANSFORMATIONS, FORCE-CONTROL, AND POSITION-CONTROL MODELS. Performance was controlled in both tasks by identical visual feedback of cursor motions on a monitor dissociated from the plane and spatial location of the motor output. Both tasks had a common goal to make ramp displacements of the cursor between targets. However, the isometric task was a force-feedback task in which the monkeys controlled cursor motion by generating forces at the hand against a rigid handle. In contrast, the movement task was a position-feedback task in which the monkeys had to move their arm and an inertial load between targets to produce the same cursor motions. In essence, the cursor became a surrogate for the moving limb that acquired the dynamical properties of the combined arm–pendulum system, and its motion on the screen was determined by the Newtonian laws of motion applied to that physical system.

Force-control models (Bushan and Shadmehr 1999; Ostry and Feldman 2003; Wolpert and Kawato 1998) assume that the motor system performs the neuronal equivalent of inverse-kinematic and inverse-dynamic transformations to convert desired cursor motions into signals that generate the appropriate limb motor outputs. In the movement task, the inverse-dynamics transformation must take into account the dynamical properties of the arm and pendulum. The directionality of M1 activity in the movement task was more closely related to the direction of measured forces at the hand than to the motion of the hand, even though the cursor displayed hand motions rather than forces. This finding would appear to implicate caudal M1 in an operation that approximates the inverse-dynamics transformation between motions and forces in Newtonian mechanics. This complements other studies that implicate M1 in a variety of transformations between extrinsic spatial and intrinsic limb- and muscle-centered parameter spaces (Battaglia-Meyer et al. 2001, 2003; Cabel et al. 2001; Caminiti et al. 1990, 1991; Gribble and Scott 2002; Kakei et al. 1999, 2001, 2003; Scott and Kalaska 1997; Sergio and Kalaska 1997, 2003).

The task-dependent changes in M1 activity might be caused by peripheral reafferent input rather than by central feedforward processes. However, those changes clearly precede the peripheral motor events, and so cannot be caused solely by feedback. The time course and timing of M1 activity also provide support for a causal role for M1 in the generation of all components of triphasic EMG responses, including the delayed "antagonist" braking pulse. Most important, it provides further neuronal foundation (Li et al. 2001; Paz et al. 2003) for behavioral evidence that the motor system can generate predictive signals to compensate for predictable changes in task dynamics (Bhushan and Shadmehr 1999; Flanagan and Wing 1997; Krouchev and Kalaska 2003; Lackner and DiZio 1994; Sainburg et al. 1995, 1999; Shadmehr and Mussa-Ivaldi 1994).

The role of M1 in feedforward compensation for task dynamics could be assessed further by comparing M1 activity in the isometric task used here, and in a second isometric task in which the cursor is given a large virtual mass and whose motion is determined by the isometric forces according to Newton's laws. The cursor's "mass" would require a transient reversal of isometric forces to decelerate it as it approached the targets. Muscle and neuronal activity should show differences between the two isometric tasks reminiscent of that seen here between the isometric and movement tasks, but without the confound of movement-dependent peripheral feedback.

Nevertheless, the present results do not constitute incontrovertible proof that M1 neurons literally solve inverse equations based on Newtonian mechanics, or that they explicitly compute hand-centered forces or joint-centered torques, before conversion to muscle activity. Likewise, although M1 activity shows clear parallels with the changes in task dynamics and EMG patterns between the two tasks, this does not prove that M1 neurons explicitly code either. It is clear, however, that M1 activity captures major features of the time course of both aspects of motor output, which are themselves closely related. As a result, the M1 motor output signal can be readily transformed into specific muscle activity patterns at the spinal level. This latter process likely involves signals that descend directly onto spinal motoneurons and others that modulate spinal reflex circuits, as well as convergent reafferent proprioceptive inputs onto both spinal populations.

Despite these caveats, the results would appear at face value to support a force-control architecture for the motor system over a position-control scheme. For instance, the "λ" model for equilibrium-point control argues that triphasic EMG patterns and complex time profiles of force outputs are generated by the interaction between descending monotonic control signals and proprioceptive feedback (Adamovitch et al. 1997; Feldman 1986; Feldman and Levin 1995; Feldman et al. 1990; Ghafouri and Feldman 2001; Gribble et al. 1998). In contrast, our findings show that the increased complexity of EMG and force outputs in the movement task is paralleled by similar increases in the temporal complexity of M1 activity. Nevertheless, our findings can still be reconciled with position-control architectures if they permitted nonmonotonic control signals in task conditions in which the viscoelastic forces generated by monotonic signals are not adequate to produce the desired kinematics. Indeed, some λ-model studies have used deviations of the control signal from the desired output kinematics, including nonmonotonic signals, to cope with task dynamics and external loads (Flash and Gurevich 1997; Gribble and Ostry 1999, 2000; Gribble et al. 1998; Latash and Gottlieb 1992; Malfait et al. 2005; Ostry and Feldman 2003). The critical distinction is in how the nonmonotonic control signals are determined. Force-control models assume an inverse-dynamics computation to explicitly plan the causal forces and torques, using knowledge of the laws of motion applied to multiarticular limbs. In contrast, equilibrium-point models produce the causal dynamics indirectly by planning a sequence of equilibrium positions, using knowledge of the dynamical properties of the musculoskeletal plant. It is not possible to ascertain whether the neuronal operations underlying the present results perform an inverse-dynamics computation in a space of Newtonian mechanical parameters or map task dynamics into a space of musculoskeletal mechanical and motoneuron-threshold parameters. However, the possibility that equilibrium-point models may permit and may even require nonmonotonic control signals to produce desired movement kinematics under conditions such as the large inertial loads used here (Flash and Gurevich 1997; Ghafouri and Feldman 2001; Gribble and Ostry 2000; Malfait et al. 2005) will make it even more difficult to distinguish between force-control and position-control architectures in neurophysiological studies.

MULTIPLE LEVELS OF REPRESENTATION. As already noted, studies have reported neuronal correlates in M1 of whole-arm task kinetics (Gribble and Scott 2002; Kalaska et al. 1989; Li et al. 2000), of transformations between extrinsic and intrinsic output parameters (Kakei et al. 1999, 2001, 2003; Scott and Kalaska 1997; Sergio and Kalaska 2003), of the spatial trajectory of limb motions (Ashe and Georgopoulos 1994; Caminiti et al. 1990, 1991; Georgopoulos et al. 1982, 1983, 1988; Kalaska et al. 1989; Moran and Schwartz 1999a,b; Reina et al. 2001; Schwartz 1992, 1993, 1994; Schwartz and Moran 1999; Schwartz et al. 1988, 2004), and of even more abstract motor output attributes in the precentral cortex (Cisek et al. 2003; Ochiai and Tanji 2002; Schwartz et al. 2004; Shen and Alexander 1997a,b). In the last studies, like the present, movement of the unseen limb was controlled by cursor motions or a video image of the arm on a monitor. Those studies found that the activity of many neurons in premotor cortex, and to a lesser degree in M1, reflected the seen motions of the visual feedback, and not the physical direction and spatial path of motion of the limb that produced those visual motions (Ochiai and Tanji 2002; Schwartz et al. 2004; Shen and Alexander 1997a,b), or even which limb controlled cursor motion (Cisek et al. 2003). M1 activity, in contrast, was more closely related to the physical motor output than premotor cortex (Cisek et al. 2003; Schwartz et al. 2004; Shen and Alexander 1997a,b).

The present study provided evidence for a further transformation in the most caudal part of M1 because the directionality of neuronal activity in the movement task deviated transiently from the direction of motion of both the controlled object (the cursor) and of the hand. Neuronal responses did not reflect the common global goal in both tasks to produce ramp displacements of the cursor between targets. It also did not reflect the dramatic difference in intended kinematics in the two tasks because the isometric task did not require any arm movements.

The evidence for multiple levels of representation across the precentral gyrus cannot be dismissed as artifacts of differences in tasks or training history because they have been found in the same animals in the same tasks (Cisek et al. 2003; Crammond

and Kalaska 2000; Johnson et al. 1996; Schwartz et al. 2004; Shen and Alexander 1997a,b). They are also consistent with spatial gradients of connectivity of different parts of the precentral gyrus with parietal and frontal cortex (Geyer et al. 2000; Johnson et al. 1996; Marconi et al. 2001; Rizzolatti and Luppino 2001).

The evidence supports the coexistence of multiple levels of motor output representation that are distributed in nonuniform fashion across the premotor and primary motor cortex. These range from abstract representations of the desired motion of a controlled object (either the limb or a surrogate such as a cursor on a screen) that are relatively independent of the peripheral plant, to progressively more limb- and joint- or muscle-centered representations of the kinematics and dynamics of motor output. Whether the transformations are distributed in a continuous gradient across the gyrus or involve more abrupt transitions between functional regions is not yet known.

REFERENCE FRAMES. The cursor displayed feedback about the measured isometric forces at the hand or hand motions. The changes in neuronal activity between tasks paralleled changes in the time course of the measured output forces at the hand. However, this does not prove that the M1 neurons were encoding motor output in a hand-centered reference frame. This study was not designed to distinguish between hand-centered and other reference frames (Kakei et al. 1999, 2001, 2003; Scott and Kalaska 1997; Sergio and Kalaska 1997, 2003). Nevertheless, several lines of evidence argue against an exclusively hand-centered framework.

First, the sampled neurons were implicated in the control of the proximal arm on the basis of several criteria (see METHODS). Proximal-arm muscles also showed the same striking changes between tasks, even though their activity is determined by the joint-centered mechanics of movement (Buneo et al. 1997; Herrmann and Flanders 1998; Kakei et al. 1999, 2001, 2003; Scott and Kalaska 1997). Nevertheless, their activity showed meaningful relations when expressed in hand-centered coordinates because the forces and torques they generate contributed indirectly to the kinematics and kinetics of motor output at the hand, transmitted through the mechanical linkage of the arm. This shows that statistical correlations with hand-centered parameters are not proof on their own of a hand-centered reference frame.

Second, there were important differences between M1 activity and the measured output forces and muscle activity. These included the initial dynamic overshoot in neuronal activity in the isometric task, the large size of the delayed "antagonist" burst of activity during movements opposite to a neuron's preferred direction compared with the size of the antagonist bursts of muscles, and the pronounced second burst of activity of many neurons after the transient pause in their preferred direction of the movement task. These prominent response transients in M1 in both tasks may be needed to drive spinal motoneurons rapidly to threshold, to quickly reset spinal reflex circuits, and to otherwise compensate for the low-pass filter properties of the motor apparatus (Ghez and Gordon 1987). Alternatively, they may reflect neuronal operations that require a transiently enhanced representation of higher-order derivatives of force output during periods of dynamic force changes, such as at the onset of motor output in each task and during movement deceleration (Georgopoulos et al. 1992; Smith et al. 1975).

Third, the magnitude of measured forces at the hand were uniform across all directions in both tasks. In contrast, there were large directional nonuniformities in M1 output signals in both tasks. The magnitude of population vectors was significantly larger for laterally directed outputs (0°, 180°) than for outputs in the orthogonal directions (90°, 270°), and the directionality of signals associated with diagonal outputs was skewed toward the lateral directions. Moreover, the transient reversal of the direction of the population vectors in the movement task was prominent in the lateral directions but much less so for the orthogonal directions. Even in the lateral directions, the trajectory of the population signal did not match exactly the trajectory of the transient reversal of measured output forces at the hand. In some cases, the forces and neuronal population vectors rotated in opposite directions during the transient reversal of output forces.

These deviations from hand-centered outputs were not a result of biased distributions of cell PDs, which were uniform in both tasks. They may partly reflect a somatotopic bias in the sample. Most neurons were related to the shoulder and shoulder girdle, with fewer related to the elbow, as in earlier studies (Kalaska et al. 1989; Scott and Kalaska 1997). The relative contributions of rotations and torques at the elbow and shoulder to endpoint motions and forces vary substantially as a function of output direction and arm geometry (Graham et al. 2003; Scott and Kalaska 1997).

Neuronal responses to sensory feedback signaling the new arm postures after each movement could also explain why there is less anisotropy in the direction and magnitude of population vectors during THT in that task compared with the isometric task, and why the THT tonic activity was similar in the two tasks even though the measured static forces were greater in the isometric task.

The anisotropic mechanical properties of the limb constitute another potential factor. The arm is inherently more stiff along the axis between the hand and shoulder than perpendicular to that axis (Gordon et al. 1994; Milner 2002; Mussa-Ivaldi et al. 1985). As a result, the inertia of the moving arm and pendulum required greater active braking forces to decelerate during lateral movements than for orthogonal directions. Furthermore, the arm approached its anatomical limits of full extension in both monkeys for movements toward the distant targets, especially 90°. Much of the braking forces measured at the handle for those movements may have been generated passively as the arm reached its anatomical limits, without activation of antagonist muscles. Similarly, for movements toward the body, the motion could be slowed in part by passive damping forces as the arm changed geometry and was drawn closer against the body. In summary, the uniform accelerating and decelerating forces measured at the hand were likely produced by different combinations of active muscular forces and internal viscoelastic factors in different directions of motor output (Gribble et al. 1998). The intrinsic anisotropies may have caused the M1 activity to deviate from the directional uniformity of measured output forces at the hand.

Finally, to perform the movement task, the motor system not only generates endpoint forces to control the motion of the inertial load of the pendulum, but must also compensate for the joint interaction torques that arise as limb segments move

relative to one another. Many neurons in caudal M1 are influenced by joint-centered dynamics parameters (Cabel et al. 2001; Gribble and Scott 2002) including neurons in the present sample (Sergio and Kalaska 1997, 2003). Compensation for interaction torques could also account for some of the directional anisotropy of the neuronal activity and deviations in the direction of rotations of forces and population vectors during the transient reversals of forces. The latter could be compounded by the fact that the recorded neuronal signals were directed to the proximal arm and any resultant joint torques were transmitted to the force transducer by the multiarticular linkage of the arm.

In summary, there is no reason to expect a perfect correspondence between the measured hand-centered output forces and the neuronal population activity. Any lack of correspondence does not refute the major findings of this study of increased temporal complexity of M1 activity in the movement task compared with the isometric task, and a transient deviation of the directionality of neuronal signals and limb motions in the movement task. Moreover, the observed anisotropies and deviations from hand-centered output parameters in both tasks provide further indirect evidence of the influence of intrinsic dynamics parameters on M1 activity.

SAMPLING BIAS. Cells were not rejected if they did not show a difference in activity in the two tasks. The only criteria for inclusion of a neuron in the study were a relation to the proximal limb, directional tuning in at least one task, and adequate isolation for the time needed to collect complete data files in both tasks. Attempts were made to sample neurons in all cortical depths but the need for recording stability for long periods of time led to a bias toward neurons with large extracellular spike amplitudes in intermediate cortical layers.

There was also a bias in the location of electrode penetrations. Most data were collected from caudal M1 in the bank of the central sulcus. The results from this study therefore should not be interpreted as a description of the canonical descending motor command to the subcortical motor apparatus. It represents only a part of that command from a specific region of M1. Other parts of M1 and the premotor cortex also contribute to the motor output command, and their contribution may have very different properties. Nevertheless, this study shows that one can record a predictive signal reflecting aspects of task dynamics in caudal M1.

IMPLICATIONS FOR NEUROPROSTHETIC CONTROLLERS. Besides any insights provided about the role of M1, this study also suggests a source of input signals to neuroprosthetic controllers to deal with a range of real-life tasks. Rapid advances are being made in brain–machine interfaces to control robotic devices (Mussa-Ivaldi and Miller 2003; Nicolelis 2003; Schwartz 2004). To date, motivated in part by neuronal studies (Georgopoulos et al. 1982, 1983, 1988; Moran and Schwartz 1999a,b; Schwartz 1992, 1993, 1994; Schwartz and Moran 1999), neuroprosthetic decoding algorithms have been designed to extract signals about the desired kinematics of motion of the robot's endpoint that can be converted into control signals to the robot's actuators (Carmena et al. 2003; Hatsopoulos et al. 2004; Paninski et al. 2004a,b; Serruya et al. 2002; Taylor et al. 2002).

To be of any practical utility, however, a prosthetic robot must interact with the world to pick up and manipulate objects, push buttons, and use tools. Its controller must be able to cope with a wide range of task dynamics in real time to produce the desired actions against the variable loads and forces presented by different tasks. However, current controllers do not switch readily between different dynamical environments without retraining (Carmena et al. 2003).

A variety of strategies could reduce this problem, such as stiff joints to minimize external perturbations and slow movements to minimize motion-dependent loads and interaction torques. Even with these measures, the controller would have to perform inverse calculations to transform the extracted endpoint kinematics signals into actuator signals to drive the robot. However, years of engineering experience have shown that implementation of a form of robotic "power steering" is a very hard real-time control problem, and that robots can be very unstable while attempting such seemingly simple tasks as exerting a constant contact force against a rigid surface.

These control problems could be reduced by exploiting the motor system's own ability to perform skillfully in many dynamical environments. These and other results show that M1 activity can provide control signals that capture the major dynamical features of tasks that transiently dissociate the directionality of arm motion from that of the causal forces and muscle activity (Gribble and Scott 2002; Li et al. 2001; Padoa-Schioppa et al. 2002, 2003) and can provide not only tonic signals that oppose the direction of a constant external load during posture and movement (Kalaska et al. 1989) but also static and dynamic signals about isometric forces generated against a rigid surface (Georgopoulos et al. 1992; Sergio and Kalaska 2003; Taira et al. 1996).

These results suggest that the most promising source of signals about task kinetics is the caudal part of M1, in the bank of the central sulcus. Appropriate decoding algorithms and training regimens in a range of task environments could greatly enhance the ability of neuroprosthetic controllers to cope with a variety of practical real-life conditions. Combined with signals about response choices and desired kinematics provided by electrode arrays implanted in motor, premotor, or parietal cortex (Cisek et al. 2003; Crammond and Kalaska 2000; Hatsopoulos et al. 2004; Kakei et al. 1999, 2001, 2003; Kalaska et al. 1989, 1990; Musallam et al. 2004; Schwartz et al. 2004), the kinetics signals extracted from caudal M1 would provide the neuroprosthetic controller with both force-control and position-control capabilities for maximum versatility.

General summary

The study of the role of the motor cortex has been dominated by debate about whether it is a low-level planner of output kinetics or a high-level planner of output goals and kinematics. Following the pioneering experiments of Evarts (1968, 1969) using a single-joint motor task, the early years of single-neuron recording studies in M1 repeatedly documented neuronal correlates of output forces and muscle activity in M1. Other controlled parametric studies, including many recent studies using whole-arm motor tasks, have reported neuronal correlates of higher-order attributes, such as the spatial trajectory of

the hand. Studies supporting these different levels of representation continue to this day (e.g., Cabel et al. 2001; Gribble and Scott 2002; Morrow and Miller 2003; Paninski et al. 2004a,b; Schwartz et al. 2004).

However, these alternatives are not necessarily mutually exclusive and incompatible. Mounting evidence suggests that motor cortex is functionally heterogeneous and that control processes at multiple levels may coexist within it. By providing evidence for predictive feedforward signals about temporal differences in task dynamics in the caudal motor cortex of monkeys that were highly skilled in two different whole-arm motor tasks requiring precise control of output forces, this study (and others, e.g., Kalaska et al. 1989; Li et al. 2001; Sergio and Kalaska 2003; Taira et al. 1996) serves to reconcile these two seemingly disparate perspectives on M1 function. It is incorrect to conclude from this study that the sole function of the motor cortex is to control output dynamics, and that representations of higher-level neuronal operations and movement attributes cannot therefore also reside in the motor cortex. The study of the motor cortex is not necessarily a zero-sum game in which only one function can be correct and all others wrong. This would be true only if the motor cortex had one specific role that involved a single homogeneous representation of motor output in a specific parameter space. The motor cortex likely has a much broader role, to contribute to the sensorimotor transformations required to convert central representations of global task goals, requirements, and constraints into signals that specify how the intended voluntary motor action can be implemented by the peripheral motor system in the current task context. This larger role not only permits but requires the presence of correlates of multiple levels of representation of motor output in M1.

ACKNOWLEDGMENTS

We thank L. Girard and N. Michaud for expert technical assistance. C. Leger (Département de Mathématiques et Statistiques, Université de Montréal) suggested the bootstrap test for significant changes in directional tuning; D. Ostry provided helpful discussions; G. Richard built the task apparatus; and R. Albert, S. Dupuis, É. Clément, C. Valiquette; and J. Jodoin provided software and electronics support.

GRANTS

This study was supported by the Canadian Institutes of Health Research (CIHR) Group Grant in Neurological Sciences (GR-15176), CIHR individual operating grants MT-14159 and MOP-62983 to J. F. Kalaska, and by postdoctoral fellowships from the Fonds de la Recherche en Santé de Québec and the Fonds pour la Formation de Chercheurs et l'Aide à la Recherche Groupe de Recherche sur le Système Nerveux Central to L. E. Sergio.

REFERENCES

Adamovich SV, Levin MF, and Feldman AG. Central modifications of reflex parameters may underlie the fastest arm movements. *J Neurophysiol* 77: 1460–1469, 1997.

Ashe J. Force and the motor cortex. *Behav Brain Res* 87: 255–269, 1997.

Ashe J and Georgopoulos AP. Movement parameters and neural activity in motor cortex and area 5. *Cereb Cortex* 4: 590–600, 1994.

Baker SN, Olivier E, and Lemon RN. Coherent oscillations in monkey motor cortex and hand muscle EMG show task-dependent modulation. *J Physiol* 501: 225–241, 1997.

Batschelet E. *Circular Statistics in Biology*. London: Academic Press, 1981.

Battaglia-Mayer A, Caminiti R, Lacquaniti F, and Zago M. Multiple levels of representation of reaching in the parieto-frontal network. *Cereb Cortex* 13: 1009–1022, 2003.

Battaglia-Mayer A, Ferraina S, Genovesio A, Marconi B, Squatrito S, Molinari M, Lacquaniti F, and Caminiti R. Eye-hand coordination during reaching. II. An analysis of the relationships between visuomanual signals in parietal cortex and parieto-frontal association projections. *Cereb Cortex* 11: 528–544, 2001.

Bennett KM and Lemon RN. The influence of single monkey cortico-motoneuronal cells at different levels of activity in target muscles. *J Physiol* 477: 291–307, 1994.

Bennett KM and Lemon RN. Corticomotoneuronal contribution to the fractionation of muscle activity during precision grip in the monkey. *J Neurophysiol* 75: 1826–1842, 1996.

Bhushan N and Shadmehr R. Computational nature of human adaptive control during learning of reaching movements in force fields. *Biol Cybern* 81: 39–60, 1999.

Bizzi E, Accornero N, Chapple W, and Hogan N. Posture control and trajectory formation during arm movement. *J Neurosci* 4: 2738–2744, 1984.

Brown SH and Cooke JD. Movement-related phasic muscle activation. I. Relations with temporal profile of movement. *J Neurophysiol* 63: 455–464, 1990.

Buneo CA, Soechting JF, and Flanders M. Muscle activation patterns for reaching: the representation of distance and time. *J Neurophysiol* 71: 1546–1558, 1994.

Buneo CA, Soechting JF, and Flanders M. Postural dependence of muscle actions: implications for neural control. *J Neurosci* 17: 2128–2142, 1997.

Buys EJ, Lemon RN, Mantel GW, and Muir RB. Selective facilitation of different hand muscles by corticospinal neurones in the conscious monkey. *J Physiol* 381: 529–549, 1986.

Cabel DW, Cisek P, and Scott SH. Neural activity in primary motor cortex related to mechanical loads applied to the shoulder and elbow during a postural task. *J Neurophysiol* 86: 2102–2108, 2001.

Caminiti R, Johnson PB, Galli C, Ferraina S, and Burnod Y. Making arm movements within different parts of space: the premotor and motor cortical representation of a coordinate system for reaching to visual targets. *J Neurosci* 11: 1182–1197, 1991.

Caminiti R, Johnson PB, and Urbano A. Making arm movements within different parts of space: dynamic aspects in the primate motor cortex. *J Neurosci* 10: 2039–2058, 1990.

Carmena JM, Lebedev MA, Crist RE, O'Doherty JE, Santucci DM, Dimitrov D, Patil PG, Henriquez CS, and Nicolelis MA. Learning to control a brain–machine interface for reaching and grasping by primates. *PLoS Biol* 1: 193–208, 2003.

Cheney PD and Fetz EE. Functional classes of primate corticomotoneuronal cells and their relation to active force. *J Neurophysiol* 44: 773–791, 1980.

Cheney PD, Fetz EE, and Palmer SS. Patterns of facilitation and suppression of antagonist forelimb muscles from motor cortex sites in the awake monkey. *J Neurophysiol* 53: 805–820, 1985.

Cisek P, Crammond DJ, and Kalaska JF. Neural activity in primary motor and dorsal premotor cortex in reaching tasks with the contralateral versus ipsilateral arm. *J Neurophysiol* 89: 922–942, 2003.

Classen J, Liepert J, Wise SP, Hallett M, and Cohen LG. Rapid plasticity of human cortical movement representation induced by practice. *J Neurophysiol* 79: 1117–1123, 1998.

Cooke JD and Brown SH. Movement-related phasic muscle activation. II. Generation and functional role of the triphasic pattern. *J Neurophysiol* 63: 465–472, 1990.

Corcos DM, Gottlieb GL, and Agarwal GC. Organizing principles for single-joint movements. II. A speed-sensitive strategy. *J Neurophysiol* 62: 358–368, 1989.

Crammond DJ and Kalaska JF. Differential relation of discharge in primary motor cortex and premotor cortex to movements versus actively maintained postures during a reaching task. *Exp Brain Res* 108: 45–61, 1996.

Crammond DJ and Kalaska JF. Prior information in motor and premotor cortex: activity during the delay period and effect on premovement activity. *J Neurophysiol* 84: 986–1005, 2000.

Drew T. Motor cortical activity during voluntary gait modifications in the cat. I. Cells related to the forelimbs. *J Neurophysiol* 70: 179–199, 1993.

Dum RP and Strick PL. Motor areas in the frontal lobe of the primate. *Physiol Behav* 77: 677–682, 2002.

Evarts EV. Relation of pyramidal tract activity to force exerted during voluntary movement. *J Neurophysiol* 31: 14–27, 1968.

Evarts EV. Activity of pyramidal tract neurons during postural fixation. *J Neurophysiol* 32: 375–385, 1969.

Feldman AG. Once more on the equilibrium-point hypothesis (Lamda Model) for motor control. *J Mot Behav* 18: 17–54, 1986.

Feldman AG, Adamovitch SV, Ostry DJ, and Flanagan JR. The origin of electromyograms—explanations based on the equilibrium point hypothesis.

In: *Multiple Muscle Systems. Biomechanics and Movement Organization*, edited by Winters JM and Woo SL-Y. New York: Springer-Verlag, 1990, p. 195–213.

Feldman AG and Levin MF. The origin and use of positional frames of reference in motor control. *Behav Brain Sci* 18: 723–744, 1995.

Fetz EE and Cheney PD. Postspike facilitation of forelimb muscle activity by primate corticomotoneuronal cells. *J Neurophysiol* 44: 751–772, 1980.

Fetz EE, Perlmutter SI, Maier MA, Flament D, and Fortier PA. Response patterns and postspike effects of premotor neurons in cervical spinal cord of behaving monkeys. *Can J Physiol Pharmacol* 74: 531–546, 1996.

Fetz EE, Perlmutter SI, and Prut Y. Functions of mammalian spinal interneurons during movement. *Curr Opin Neurobiol* 10: 699–707, 2000.

Flanagan JR and Wing AM. The role of internal models in motion planning and control: evidence from grip force adjustments during movements of hand-held loads. *J Neurosci* 17: 1519–1528, 1997.

Flanders M. Temporal patterns of muscle activation for arm movements in three-dimensional space. *J Neurosci* 11: 2680–2693, 1991.

Flash T and Gurevich I. Models of motor adaptation and impedance control in human arm movements. In: *Self-Organization, Computational Maps and Motor Control*, edited by Morasso P and Sanguineti V. Amsterdam: Springer/North-Holland, 1997, p. 423–481.

Forget R and Lamarre Y. Rapid elbow flexion in the absence of proprioceptive and cutaneous feedback. *Hum Neurobiol* 6: 27–37, 1987.

Fu QG, Flament D, Coltz JD, and Ebner TJ. Temporal encoding of movement kinematics in the discharge of primate primary motor and premotor neurons. *J Neurophysiol* 73: 836–854, 1995.

Fu QG, Suarez JI, and Ebner TJ. Neuronal specification of direction and distance during reaching movements in the superior precentral premotor area and primary motor cortex of monkeys. *J Neurophysiol* 70: 2097–2116, 1993.

Gandolfo F, Mussa-Ivaldi FA, and Bizzi E. Motor learning by field approximation. *Proc Natl Acad Sci USA* 93: 3843–3846, 1996.

Georgopoulos AP, Ashe J, Smyrnis N, and Taira M. The motor cortex and the coding of force. *Science* 256: 1692–1695, 1992.

Georgopoulos AP, Caminiti R, Kalaska JF, and Massey JT. Spatial coding of movement: a hypothesis concerning the coding of movement direction by motor cortical populations. In: *Neural Coding of Motor Performance*, edited by Massion J, Paillard J, Schultz W, and Wiesendanger M. *Exp Brain Res Suppl* 7: 327–336, 1983.

Georgopoulos AP, Kalaska JF, Caminiti R, and Massey JT. On the relations between the direction of two-dimensional arm movements and cell discharge in primate motor cortex. *J Neurosci* 2: 1527–1537, 1982.

Georgopoulos AP, Kettner RE, and Schwartz AB. Primate motor cortex and free-arm movements to visual targets in three-dimensional space. II. Coding of the direction of movement by a neuronal population. *J Neurosci* 8: 2931–2937, 1988.

Geyer S, Matelli M, Luppino G, and Zilles K. Functional neuroanatomy of the primate isocortical motor system. *Anat Embryol* (*Berl*) 202: 443–474, 2000.

Ghafouri M and Feldman AG. The timing of control signals underlying fast point-to-point arm movements. *Exp Brain Res* 137: 411–423, 2001.

Ghez C and Gordon J. Trajectory control in targeted force impulses. I. Role of opposing muscles. *Exp Brain Res* 67: 225–240, 1987.

Ghez C and Martin JH. The control of rapid limb movement in the cat. III. Agonist–antagonist coupling. *Exp Brain Res* 45: 115–125, 1982.

Gordon J, Ghilardi MF, Cooper SE, and Ghez C. Accuracy of planar reaching movements. II. Systematic extent errors resulting from inertial anisotropy. *Exp Brain Res* 99: 112–130, 1994.

Gottlieb GL, Corcos DM, and Agarwal GC. Organizing principles for single-joint movements. I. A speed-insensitive strategy. *J Neurophysiol* 62: 342–357, 1989.

Graham KM, Moore KD, Cabel WD, Gribble PL, Cisek P, and Scott SH. Kinematics and kinetics of multijoint reaching in nonhuman primates. *J Neurophysiol* 89: 2667–2677, 2003.

Gribble PL and Ostry DJ. Independent coactivation of shoulder and elbow muscles. *Exp Brain Res* 123: 355–360, 1998.

Gribble PL and Ostry DJ. Compensation for interaction torques during single- and multi-joint limb movement. *J Neurophysiol* 82: 2310–2326, 1999.

Gribble PL and Ostry DJ. Compensation for loads during arm movements using equilibrium control. *Exp Brain Res* 135: 474–482, 2000.

Gribble PL, Ostry DJ, Sanguineti V, and Laboissiere R. Are complex control signals required for human arm movement? *J Neurophysiol* 79: 1409–1424, 1998.

Gribble PL and Scott SH. Overlap of internal models in motor cortex for mechanical loads during reaching. *Nature* 417: 938–941, 2002.

Hallett M, Shahani BT, and Young RR. EMG analysis of stereotyped voluntary movements in man. *J Neurol Neurosurg Psychiatry* 38: 1154–1162, 1975.

Haruno M, Wolpert DM, and Kawato M. Mosaic model for sensorimotor learning and control. *Neural Comput* 13: 2201–2220, 2001.

Hatsopoulos N, Joshi J, and O'Leary JG. Decoding continuous and discrete motor behaviors using motor and premotor cortical ensembles. *J Neurophysiol* 92: 1165–1174, 2004.

He SQ, Dum RP, and Strick PL. Topographic organization of corticospinal projections from the frontal lobe: motor areas on the lateral surface of the hemisphere. *J Neurosci* 13: 952–980, 1993.

Hepp-Reymond M, Kirkpatrick-Tanner M, Gabernet L, Qi HX, and Weber B. Context-dependent force coding in motor and premotor cortical areas. *Exp Brain Res* 128: 123–133, 1999.

Herrmann U and Flanders M. Directional tuning of single motor units. *J Neurosci* 18: 8402–8416, 1998.

Hoffman DS and Luschei ES. Responses of monkey precentral cortical cells during a controlled jaw bite task. *J Neurophysiol* 44: 333–348, 1980.

Hoffman DS and Strick PL. Step-tracking movements of the wrist. IV. Muscle activity associated with movements in different directions. *J Neurophysiol* 81: 319–333, 1999.

Holdefer RN and Miller LE. Primary motor cortical neurons encode functional muscle synergies. *Exp Brain Res* 146: 233–243, 2002.

Hollerbach JM. Computers, brains and the control of movement. *Trends Neurosci* 6: 189–192, 1982.

Hollerbach JM and Flash T. Dynamic interactions between limb segments during planar arm movement. *Biol Cybern* 44: 67–77, 1982.

Humphrey DR, Schmidt EM, and Thompson WD. Predicting measures of motor performance from multiple cortical spike trains. *Science* 170: 758–762, 1970.

Johnson PB, Ferraina S, Bianchi L, and Caminiti R. Cortical networks for visual reaching: physiological and anatomical organization of frontal and parietal lobe arm regions. *Cereb Cortex* 6: 102–119, 1996.

Kakei S, Hoffman DS, and Strick PL. Muscle and movement representations in the primary motor cortex. *Science* 285: 2136–2139, 1999.

Kakei S, Hoffman DS, and Strick PL. Direction of action is represented in the ventral premotor cortex. *Nat Neurosci* 4: 1020–1025, 2001.

Kakei S, Hoffman DS, and Strick PL. Sensorimotor transformations in cortical motor areas. *Neurosci Res* 46: 1–10, 2003.

Kalaska JF, Cohen DA, Hyde ML, and Prud'homme M. A comparison of movement direction-related versus load direction-related activity in primate motor cortex, using a two-dimensional reaching task. *J Neurosci* 9: 2080–2102, 1989.

Kalaska JF, Cohen DA, Prud'homme M, and Hyde ML. Parietal area 5 neuronal activity encodes movement kinematics, not movement dynamics. *Exp Brain Res* 80: 351–364, 1990.

Kargo WJ and Nitz DA. Early skill learning is expressed through selection and tuning of cortically represented muscle synergies. *J Neurosci* 23: 11255–11269, 2003.

Kargo WJ and Nitz DA. Improvements in the signal-to-noise ratio of motor cortex cells distinguishes early versus late phases of motor skill learning. *J Neurosci* 24: 5560–5569, 2004.

Karst GM and Hasan Z. Initiation rules for planar, two-joint arm movements: agonist selection for movements throughout the work space. *J Neurophysiol* 66: 1579–1593, 1991a.

Karst GM and Hasan Z. Timing and magnitude of electromyographic activity for two-joint arm movements in different directions. *J Neurophysiol* 66: 1594–1604, 1991b.

Koshland GF, Galloway JC, and Nevoret-Bell CJ. Control of the wrist in three-joint arm movements to multiple directions in the horizontal plane. *J Neurophysiol* 83: 3188–3195, 2000.

Krouchev NI and Kalaska JF. Context-dependent anticipation of different task dynamics: rapid recall of appropriate motor skills using visual cues. *J Neurophysiol* 89: 1165–1175, 2003.

Lackner JR and DiZio P. Rapid adaptation to coriolis force perturbations of arm trajectory. *J Neurophysiol* 72: 299–313, 1994.

Latash ML and Gottlieb GL. Virtual trajectories of single-joint movements performed under two basic strategies. *Neuroscience* 47: 357–365, 1992.

Lemon RN and Mantel GW. The influence of changes in discharge frequency of corticospinal neurones on hand muscles in the monkey. *J Physiol* 413: 351–378, 1989.

Li CS, Padoa-Schioppa C, and Bizzi E. Neuronal correlates of motor performance and motor learning in the primary motor cortex of monkeys adapting to an external force field. *Neuron* 30: 593–607, 2001.

Loeb EG. Hard lessons in motor control from the mammalian spinal cord. *Trends Neurosci* 10: 108–113, 1987.

Maier MA, Bennett KM, Hepp-Reymond MC, and Lemon RN. Contribution of the monkey corticomotoneuronal system to the control of force in precision grip. *J Neurophysiol* 69: 772–785, 1993.

Malfait N, Gribble PB, and Ostry DJ. Generalization of motor learning based on multiple field exposures and local adaptation. *J Neurophysiol* 93: 3327–3338, 2005.

Marconi B, Genovesio A, Battaglia-Mayer A, Ferraina S, Squatrito S, Molinari M, Lacquaniti F, and Caminiti R. Eye-hand coordination during reaching. I. Anatomical relationships between parietal and frontal cortex. *Cereb Cortex* 11: 513–527, 2001.

Milner TE. Contribution of geometry and joint stiffness to mechanical stability of the human arm. *Exp Brain Res* 143: 515–519, 2002.

Moran DW and Schwartz AB. Motor cortical representation of speed and direction during reaching. *J Neurophysiol* 82: 2676–2692, 1999a.

Moran DW and Schwartz AB. Motor cortical activity during drawing movements: population representation during spiral tracing. *J Neurophysiol* 82: 2693–2704, 1999b.

Morrow MM and Miller LE. Prediction of muscle activity by populations of sequentially recorded primary motor cortex neurons. *J Neurophysiol* 89: 2279–2288, 2003.

Muir RB and Lemon RN. Corticospinal neurons with a special role in precision grip. *Brain Res* 261: 312–316, 1983.

Musallam S, Corneil BD, Greger B, Scherberger H, and Andersen RA. Cognitive control signals for neural prosthetics. *Science* 305: 258–262, 2004.

Mussa-Ivaldi FA, Hogan N, and Bizzi E. Neural, mechanical, and geometric factors subserving arm posture in humans. *J Neurosci* 5: 2732–2743, 1985.

Mussa-Ivaldi FA and Miller LE. Brain-machine interfaces: computational demands and clinical needs meet basic neuroscience. *Trends Neurosci* 26: 329–334, 2003.

Nakano E, Imamizu H, Osu R, Uno Y, Gomi H, Yoshioka T, and Kawato M. Quantitative examinations of internal representations for arm trajectory planning: minimum commanded torque change model. *J Neurophysiol* 81: 2140–2155, 1999.

Nicolelis MA. Brain-machine interfaces to restore motor function and probe neural circuits. *Nat Rev Neurosci* 4: 417–422, 2003.

Nudo RJ, Milliken GW, Jenkins WM, and Merzenich MM. Use-dependent alterations of movement representations in primary motor cortex of adult squirrel monkeys. *J Neurosci* 16: 785–807, 1996.

Ochiai T, Mushiake H, and Tanji J. Effects of image motion in the dorsal premotor cortex during planning of an arm movement. *J Neurophysiol* 88: 2167–2171, 2002.

Ostry DJ and Feldman AG. A critical evaluation of the force control hypothesis in motor control. *Exp Brain Res* 153: 275–288, 2003.

Padoa-Schioppa C, Li CS, and Bizzi E. Neuronal correlates of kinematics-to-dynamics transformation in the supplementary motor area. *Neuron* 36: 751–765, 2002.

Padoa-Schioppa C, Li CS, and Bizzi E. Neuronal activity in the supplementary motor area of monkeys adapting to a new dynamic environment. *J Neurophysiol* 91: 449–473, 2003.

Paninski L, Fellows MR, Hatsopoulos NG, and Donoghue JP. Spatiotemporal tuning of motor cortical neurons for hand position and velocity. *J Neurophysiol* 91: 515–532, 2004a.

Paninski L, Shohan S, Fellows MR, Hatsopoulos N, and Donoghue JP. Superlinear population encoding of dynamic hand trajectory in primary motor cortex. *J Neurosci* 29: 8551–8561, 2004b.

Park MC, Belhaj-Saif A, and Cheney PD. Properties of primary motor cortex output to forelimb muscles in rhesus monkeys. *J Neurophysiol* 92: 2968–2984, 2004.

Paz R, Boraud T, Natan C, Bergman H, and Vaadia E. Preparatory activity in motor cortex reflects learning of local visuomotor skills. *Nat Neurosci* 6: 882–890, 2003.

Paz R and Vaadia E. Learning-induced improvement in encoding and decoding of specific movement directions by neurons in primary motor cortex. *PLoS Biol* 2: 264–274, 2004.

Poliakov AV and Schieber MH. Limited functional grouping of neurons in the motor cortex hand area during individuated finger movements: a cluster analysis. *J Neurophysiol* 82: 3488–3505, 1999.

Polit A and Bizzi E. Characteristics of motor programs underlying arm movements in monkeys. *J Neurophysiol* 42: 183–194, 1979.

Reina GA, Moran DW, and Schwartz AB. On the relationship between joint angular velocity and motor cortical discharge during reaching. *J Neurophysiol* 85: 2576–2589, 2001.

Rioult-Pedotti MS, Friedman D, Hess G, and Donoghue JP. Strengthening of horizontal cortical connections following skill learning. *Nat Neurosci* 1: 230–234, 1998.

Rizzolatti G and Luppino G. The cortical motor system. *Neuron* 31: 889–901, 2001.

Sainburg RL, Ghez C, and Kalakanis D. Intersegmental dynamics are controlled by sequential anticipatory, error correction, and postural mechanisms. *J Neurophysiol* 81: 1045–1056, 1999.

Sainburg RL, Ghilardi MF, Poizner H, and Ghez C. Control of limb dynamics in normal subjects and patients without proprioception. *J Neurophysiol* 73: 820–835, 1995.

Schieber MH and Poliakov AV. Partial inactivation of the primary motor cortex hand area: effects on individuated finger movements. *J Neurosci* 18: 9038–9054, 1998.

Schwartz AB. Motor cortical activity during drawing movements: single-unit activity during sinusoid tracing. *J Neurophysiol* 68: 528–541, 1992.

Schwartz AB. Motor cortical activity during drawing movements: population representation during sinusoid tracing. *J Neurophysiol* 70: 28–36, 1993.

Schwartz AB. Direct cortical representation of drawing. *Science* 265: 540–542, 1994.

Schwartz AB. Cortical neural prosthetics. *Ann Rev Neurosci* 27: 487–507, 2004.

Schwartz AB, Kettner RE, and Georgopoulos AP. Primate motor cortex and free-arm movements to visual targets in three-dimensional space. I. Relations between single cell discharge and direction of movement. *J Neurosci* 8: 2913–2927, 1988.

Schwartz AB and Moran DW. Motor cortical activity during drawing movements: population representation during lemniscate tracing. *J Neurophysiol* 82: 2705–2718, 1999.

Schwartz AB, Moran DW, and Reina GA. Differential representation of perception and action in the frontal cortex. *Science* 303: 380–383, 2004.

Schweighofer N, Arbib MA, and Kawato M. Role of the cerebellum in reaching movements in humans. I. Distributed inverse dynamics control. *Eur J Neurosci* 10: 86–94, 1998.

Scott SH and Kalaska JF. Temporal changes in the effect of arm orientation on directional tuning of cells in monkey primary motor (M1) and dorsal premotor (PMd) cortex during reaching. *Soc Neurosci Abstr* 22: 1829, 1996.

Scott SH and Kalaska JF. Reaching movements with similar hand paths but different arm orientations. I. Activity of individual cells in motor cortex. *J Neurophysiol* 77: 826–852, 1997.

Scott SH, Sergio LE, and Kalaska JF. Reaching movements with similar hand paths but different arm orientations. II. Activity of individual cells in dorsal premotor cortex and parietal area 5. *J Neurophysiol* 78: 2413–2426, 1997.

Sergio LE and Kalaska JF. Systematic changes in directional tuning of motor cortex cell activity with hand location in the workspace during generation of static isometric forces in constant spatial directions. *J Neurophysiol* 78: 1170–1174, 1997.

Sergio LE and Kalaska JF. Changes in the temporal pattern of primary motor cortex activity in a directional isometric force versus limb movement task. *J Neurophysiol* 80: 1577–1583, 1998.

Sergio LE and Kalaska JF. Systematic changes in motor cortex cell activity with arm posture during directional isometric force generation. *J Neurophysiol* 89: 212–228, 2003.

Serruya MD, Hatsopoulos NG, Paninski L, Fellows MR, and Donoghue JP. Instant neural control of a movement signal. *Nature* 416: 141–142, 2002.

Shadmehr R and Moussavi ZM. Spatial generalization from learning dynamics of reaching movements. *J Neurosci* 20: 7807–7815, 2000.

Shadmehr R and Mussa-Ivaldi FA. Adaptive representation of dynamics during learning of a motor task. *J Neurosci* 14: 3208–3224, 1994.

Shen L and Alexander GE. Neural correlates of a spatial sensory-to-motor transformation in primary motor cortex. *J Neurophysiol* 77: 1171–1194, 1997a.

Shen L and Alexander GE. Preferential representation of instructed target location versus limb trajectory in dorsal premotor area. *J Neurophysiol* 77: 1195–1212, 1997b.

Smith AM, Hepp-Reymond MC, and Wyss UR. Relation of activity in precentral cortical neurons to force and rate of force change during isometric contractions of finger muscles. *Exp Brain Res* 23: 315–332, 1975.

Taira M, Boline J, Smyrnis N, Georgopoulos AP, and Ashe J. On the relations between single cell activity in the motor cortex and the direction and magnitude of three-dimensional static isometric force. *Exp Brain Res* 109: 367–376, 1996.

Taylor DM, Tillery SI, and Schwartz AB. Direct cortical control of 3D neuroprosthetic devices. *Science* 296: 1829–1832, 2002.

Thach WT. Correlation of neural discharge with pattern and force of muscular activity, joint position, and direction of intended next movement in motor cortex and cerebellum. *J Neurophysiol* 41: 654–676, 1978.

Thoroughman KA and Shadmehr R. Electromyographic correlates of learning an internal model of reaching movements. *J Neurosci* 19: 8573–8588, 1999.

Thoroughman KA and Shadmehr R. Learning of action through adaptive combination of motor primitives. *Nature* 407: 742–747, 2000.

Todorov E. Direct cortical control of muscle activation in voluntary arm movements: a model. *Nat Neurosci* 3: 391–398, 2000.

Uno Y, Kawato M, and Suzuki R. Formation and control of optimal trajectory in human multijoint arm movement. Minimum torque-change model. *Biol Cybern* 61: 89–101, 1989.

Wadman WJ, Denier van der Gon JJ, and Derksen RJA. Muscle activation patterns for fast goal-directed arm movements. *J Hum Movement Stud* 6: 19–37, 1980.

Werner W, Bauswein E, and Fromm C. Static firing rates of premotor and primary motor cortical neurons associated with torque and joint position. *Exp Brain Res* 86: 293–302, 1991.

Wise SP, di Pelligrino G, and Boussaoud D. The premotor cortex and nonstandard sensorimotor mapping. *Can J Physiol Pharmacol* 74: 469–482, 1996.

Wolpert DM and Kawato M. Multiple paired forward and inverse models for motor control. *Neural Networks* 11: 1317–1329, 1998.

Zajac FE and Gordon ME. Determining muscle's force and action in multi-articular movement. *Exerc Sport Sci Rev* 17: 187–230, 1989.

Zhang J, Riehle A, Requin J, and Kornblum S. Dynamics of single neuron activity in monkey primary motor cortex related to sensorimotor transformation. *J Neurosci* 17: 2227–2246, 1997.